

Structural Diversity in Supramolecular Organization of Anionic Phosphate Monoesters: Role of Cations

Biswajit Santra,[†] Debdeep Mandal,[†] Vivek Gupta,[†] Pankaj Kalita,[‡] Vierandra Kumar,[§] Ramakirushnan Suriya Narayanan,[†] Atanu Dey,[†] Nicolas Chrysochos,^{||} Akbar Mohammad,[⊥] Ajeet Singh,[⊥] Michael Zimmer,[#] Rana Dalapati,[∇] Shyam Biswas,^{*,∇} Carola Schulzke,^{*,||} Vadapalli Chandrasekhar,^{*,†,§} David Scheschkewitz,^{*,#} and Anukul Jana^{*,†}

[†]Tata Institute of Fundamental Research Hyderabad, Gopanally, Hyderabad 500107, India

[‡]National Institute of Science Education and Research Bhubaneswar, HBNI, Bhubaneswar 752050, Odisha, India

[§]Department of Chemistry, Indian Institute of Technology Kanpur, Kanpur 208016, India

^{||}Institut für Biochemie, Ernst-Moritz-Arndt Universität Greifswald, Felix-Hausdorff-Straße 4, D-17487 Greifswald, Germany

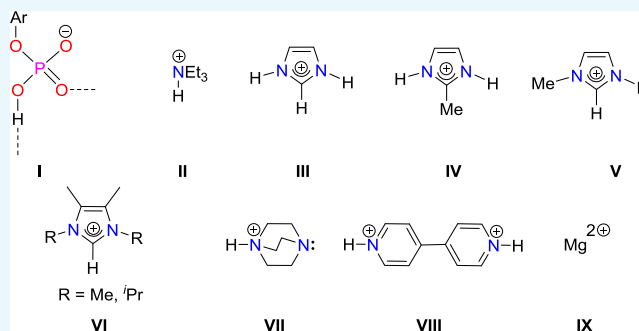
[⊥]Discipline of Chemistry, Indian Institute of Technology Indore, Simrol, Khandwa Road, Indore 453552, India

[#]Krupp-Chair of General and Inorganic Chemistry, Saarland University, 66123 Saarbrücken, Germany

[∇]Department of Chemistry, Indian Institute of Technology Guwahati, Guwahati 781039, Assam, India

Supporting Information

ABSTRACT: Syntheses and structures of anionic arylphosphate monoesters [ArOP(O)₂(OH)][−] (Ar = 2,6-CHPh₂-4-R-C₆H₂; R = Me/Et/*i*Pr/*t*Bu) with different counter cations are reported. The counter cations were varied systematically: imidazolium cation, 2-methyl imidazolium cation, *N*-methyl imidazolium cation, *N,N'*-alkyl substituted imidazolium cation, 1,4-diazabicyclo[2.2.2]octan-1-ium cation, 4,4'-bipyridinium dication, and magnesium(II) dication. The objective was to examine if the supramolecular structure of anionic arylphosphate monoesters could be modulated by varying the cation. It was found that an eight-membered P₂O₄H₂-hydrogen-bonded dimeric motif involving intermolecular H-bonding between the [P(O)(OH)] unit of the anionic phosphate monoester along with the counter cation is formed with 2-methyl imidazolium cation, *N*-methyl imidazolium cation, *N,N'*-alkyl substituted imidazolium cation, 1,4-diazabicyclo[2.2.2]octan-1-ium cation, and magnesium(II) dication; both discrete and polymeric H-bonded structures are observed. In the case of imidazolium cations and 1,4-diazabicyclo[2.2.2]octan-1-ium cation, the formation of one-dimensional polymers (single lane/double lane) was observed. On the other hand, two types of phosphate motifs, intermolecular H-bonded dimer and an open-form, were observed in the case of 4,4'-bipyridinium dication.



1. INTRODUCTION

Noncovalent interactions such as hydrogen bonding, π - π stacking, van der Waals interactions, and electrostatic interactions play an important role in one-dimensional (1D), two-dimensional (2D), and three-dimensional supramolecular assemblies of various compounds.^{1,2} In particular, hydrogen bonding is crucial for the structural evolution and for the associated properties in both biological and nonbiological settings.³ In living organisms, the phosphate functional group, OP(O)(OH)₂, is a ubiquitous structural element known to participate in H-bonding with a variety of functional groups, leading to exquisite control of the biological activities.⁴ In organic synthesis, particularly in the field of Brønsted acid-catalyzed organocatalysis, chiral phosphatediesters (e.g., binol-based phosphatediesters) are well established.^{5–7} The H-bonding of the chiral phosphate diesters with the substrate

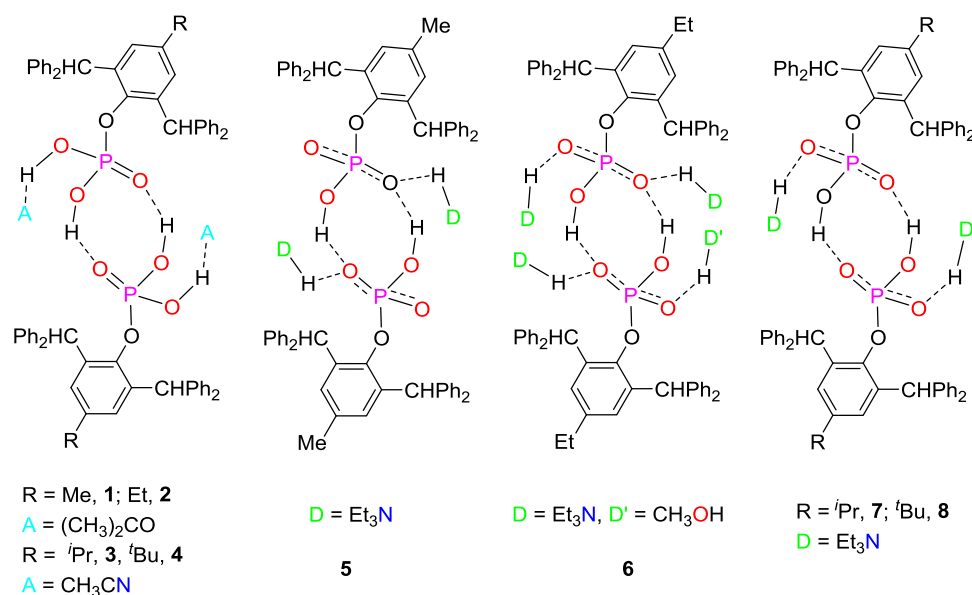
leads to significant enantiomeric excess.^{8–13} Similar applications have been reported in asymmetric fluorination^{14,15} and in the case of Heck–Matsuda coupling reactions.¹⁶ In this context, we became interested in the reaction of phosphate monoesters with different bases to study the H-bonding interaction of the resulting ion pair between an anionic phosphate monoester and different counter cations. Although molecular phosphate monoesters mostly form polymeric structures in the solid state,^{17–25} we have recently reported the syntheses of several bulky aryl-substituted neutral and anionic phosphate monoesters (1–8 in Scheme 1), which exhibit H-bonded dimeric molecular structures analogous to

Received: November 15, 2018

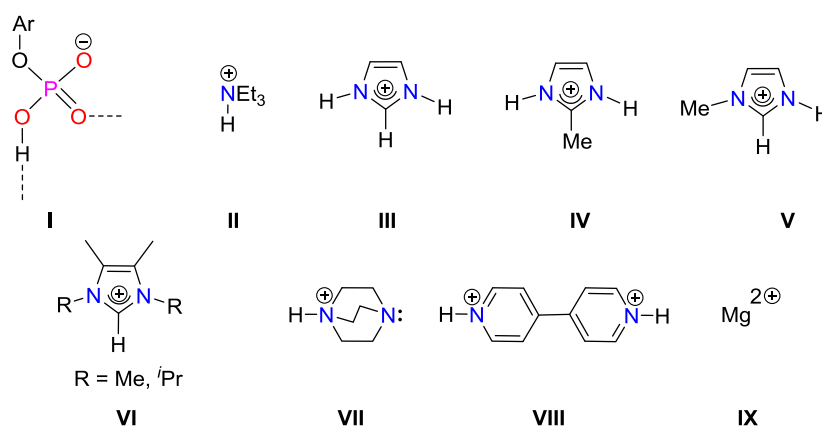
Accepted: January 2, 2019

Published: January 29, 2019

Scheme 1. Chemical Structures of Dimeric Forms of Neutral Aryl Phosphate Monoesters, 1–4 and Anionic Aryl Phosphate Monoesters along with Et_3NH^+ as Counter Cation, 5–8²⁶



Scheme 2. Chemical Structures of Anionic Phosphate Monoester I, Monocations II–VII, and Dications VIII–IX



those in carboxylic acids.²⁶ Through partial blockage of the H-bonding potential of the $\text{ArOP}(\text{O})(\text{OH})_2$ unit by using either a hydrogen-bonding acceptor solvent (such as acetone or acetonitrile) or a hydrogen-bonding donor as counter cation (such as triethylammonium), we were able to realize dimeric supramolecular structures (Scheme 1). Murugavel et al. independently also reported the synthesis and molecular structures of 1 and 4.²⁷

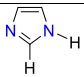
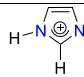
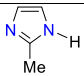
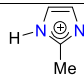
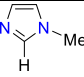
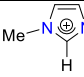
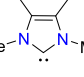
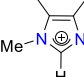
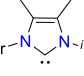
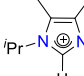
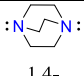
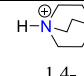
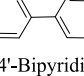
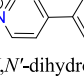
In the case of the neutral phosphate monoesters 1–4, the $\text{P}(\text{O})(\text{OH})_2$ unit is engaged in an eight-membered $\text{P}_2\text{O}_4\text{H}_2$ -hydrogen-bonded dimer leaving the remaining $\text{P}-\text{OH}$ moiety for H-bonding with the solvent (Scheme 1). On the other hand, in the anionic phosphate monoesters, 5–8, the H-bonding in the dimeric structure varies with the substituent in para-position. Thus, in 5, the terminal $\text{P}=\text{O}$ is free, while in 7 and 8, it is involved in H-bonding interaction with the triethylammonium counter cation.

The above findings were limited to the triethylammonium counter cation II. It was therefore of interest to systematically study the structures of various self-assembled anionic phosphate monoesters I with different types of counter cations to gauge their effect on the supramolecular organization of the

anionic phosphate monoesters. Accordingly, we chose different monocations and dications in an anticipation to induce a larger structural diversity (Scheme 2): imidazolium cation III, 2-methyl imidazolium cation IV, *N*-methyl imidazolium cation V, *N,N'*-dialkyl-imidazolium cation VI, 1,4-diazabicyclo[2.2.2]octan-1-ium cation VII, *N,N'*-dihydro-4,4'-bipyridinium dication VIII, and magnesium dication IX (Scheme 2).

Thus, families of ion pairs containing anionic phosphate monoesters with various counter cations (III, IV, V, VI, and VII) were obtained by the stoichiometric reaction of the phosphate monoesters with imidazole, *N*-methyl imidazole, *N,N'*-dialkyl-imidazol-2-ylidene (*N*-heterocyclic carbene, NHC), and 1,4-diazabicyclo[2.2.2]octane (DABCO), respectively. The anionic phosphate monoesters with counter cations VIII and IX were obtained by a 2:1 reaction of the phosphate monoesters with 4,4'-bipyridine and magnesium dichloride in the presence of Et_3N . Apart from balancing the counter charge of phosphate monoesters, the employed cations have different numbers of potential H-bonding sites available, which was expected to lead to different supramolecular structures (Table 1). While the imidazolium cation III possesses two *N*-H units along with a $\text{C}2-\text{H}$ unit as H-bonding donor, the 2-methyl-

Table 1. Overview of the Resulting Structures of Different Phosphate Ion Pairs

Phosphatemonoester	Source of Cation	Active Cationic Species	presence of H-bonding donor/acceptor unit(s) in the active cationic species	Involvement of Solvent(s) in H-bonding	Resulting Structure
4	 Imidazole	 Imidazolium cation, III	two N-H donor one C-H donor	DMF	1-D double lane polymer (9)
3	 2-Methylimidazole	 2-Methylimidazolium cation, IV	two N-H donor	-	1-D double lane polymer (10)
3	 <i>N</i> -Methylimidazole	 <i>N</i> -Methylimidazolium cation, V	N-H donor C-H donor	MeOH	Discrete dimer (11)
4	 1,3,4,5-tetramethylimidazol-2-ylidene	 1,3,4,5-tetramethylimidazolium cation, VI	C-H donor	-	Discrete dimer (12)
4	 1,3-diisopropyl-4,5-dimethylimidazol-2-ylidene	 1,3-diisopropyl-4,5-dimethylimidazolium cation, VI	C-H donor	-	Discrete dimer (13)
1	 1,4-diazabicyclo[2.2.2]octane (DABCO)	 1,4-diazabicyclo[2.2.2]octan-1-ium cation VII	N-H donor N: acceptor	CH ₃ OH, H ₂ O, and DMF	1-D polymer (14)
3	 4,4'-Bipyridine	 <i>N,N'</i> -dihydro-4,4'-bipyridinium dication, VIII	two N-H donor	CH ₃ OH and H ₂ O	1-D polymer (15)
2	MgCl ₂ /Et ₃ N	Mg ²⁺ IX			1-D polymer (16)
3	MgCl ₂ /Et ₃ N	Mg ²⁺ IX			Discrete dimer (17)

imidazolium cation **IV** has only two *N*-H units accessible for this purpose. In contrast, the *N*-methyl-imidazolium cation **V** features just a single *N*-H unit along with a C2-H unit as donor for H-bonding interaction. The *N,N'*-alkyl-substituted imidazolium cation can be considered as similar to a triethylammonium cation, where the C2-H can serve as a H-bond donor. 1,4-Diazabicyclo[2.2.2]octan-1-ium cation **VII** has one *N*-H moiety as a potential H-bond donor, but in

addition, a tertiary *N* center as a H-bond acceptor. The *N,N'*-dihydro-4,4'-bipyridinium dication **VIII** is characterized by two *N*-H donor centers separated by a rigid spacer; the possibility of the formation of an H-bonded polymer can be envisaged. Finally, the magnesium dication (Mg²⁺) **IX** on its own would only neutralize the charge of the anionic phosphate monoester, but not participate in H-bonding (Scheme 2).

Scheme 3. Synthesis of 9

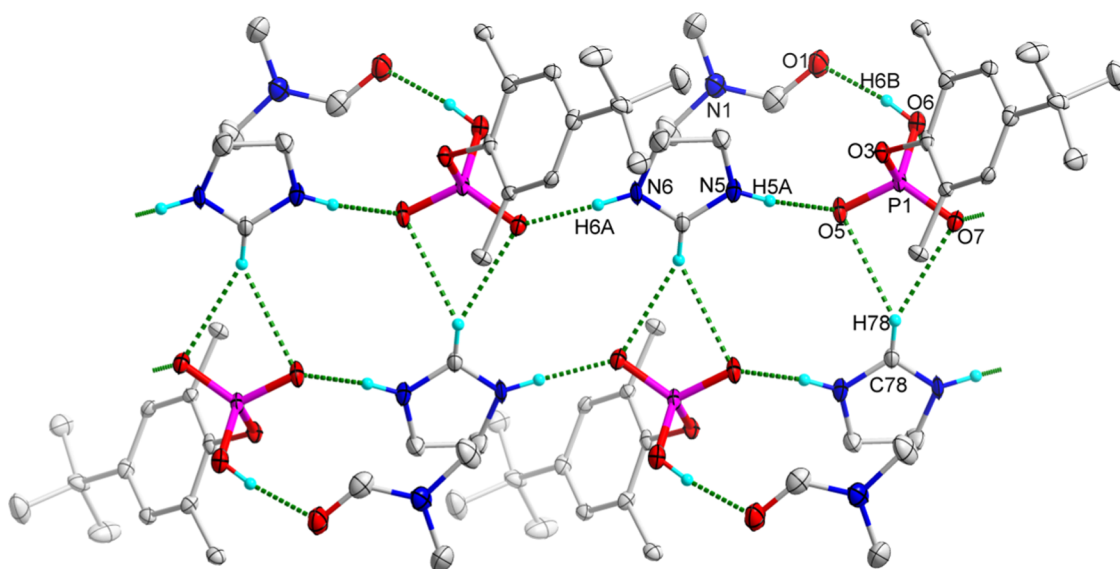
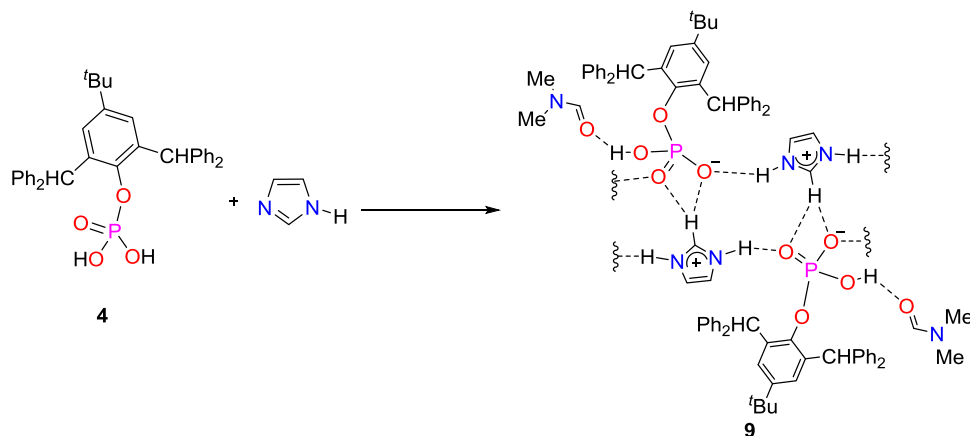


Figure 1. H-bonded supramolecular structure of **9** with thermal ellipsoids of 50% probability. Selected bond lengths (Å) and bond angles (deg): P(1)–O(5) 1.4923(3), P(1)–O(7) 1.4868(3), P(1)–O(6) 1.5727(3), O(7)–P(1)–O(6) 107.79(2), O(7)–P(1)–O(5) 118.29(2), O(6)–P(1)–O(5) 111.74(2). Selected H-bond distances (Å) and angles (deg): O(7)⋯N(6) 2.6451(4), H(6A)⋯O(7) 1.8027(3), N(6)–H(6A)⋯O(7) 166.01(2), N(5)⋯O(5) 2.6678(5), H(5A)⋯O(5) 1.8252(3), N(5)–H(5A)⋯O(5) 165.89(3), O(6)⋯O(1) 2.6160(4), H(6B)⋯O(1) 1.8353(3), O(6)–H(6B)⋯O(1) 158.63(2), C(78)⋯O(5) 3.365(5), H(78)⋯O(5) 2.665(3), C(78)–H(78)⋯O(7) 132.59(3), C(78)⋯O(7) 3.317(5), H(78)⋯O(7) 2.507(3), C(78)–H(78)⋯O(7) 145.59(3).

2. RESULTS AND DISCUSSION

2.1. Synthesis and Molecular Characterization. In the current study, we investigated our recently reported bulky aryl-substituted phosphate monoesters, ArOP(O)(OH)₂ (Ar = 2,6-CHPh₂-4-R-C₆H₂; R = Me, **1**; Et, **2**; *i*Pr, **3**; and *t*Bu, **4**), as a source of the anionic phosphate monoester, **I**. The reaction of **4** with 1 equiv of imidazole in CH₃CN led to a white precipitate after stirring the reactants for 20 h at room temperature (Scheme 3). The resulting solid was crystallized in a 1:1 dimethylformamide (DMF)/CH₃OH solution at room temperature, affording pure crystals of **9** (76% yield), which were suitable for single-crystal X-ray diffraction analysis.

Solid-state molecular structure analysis reveals that **9** crystallizes along with DMF as a solvent molecule. The three donor units of the imidazolium cation take part in H-bonding with an anionic phosphate unit. The C2–H of the imidazolium moiety is involved in a bifurcated H-bond with PO₂[−]. Here, the C2 carbon referred to the carbon center of imidazole/imidazolium moiety, which has been flanked between two N

centers. The two N–H moieties of the imidazolium cation each show slightly bent H-bonding with P–O units of two adjacent anionic phosphate monoesters resulting in the formation of a 1D H-bonded network. Additionally, the P–O–H moiety of the anionic phosphate moiety is involved in intermolecular H-bonding with the carbonyl group of DMF (Figure 1). The ³¹P{¹H} solution NMR spectrum of **9** shows a singlet at δ = −4.7 ppm, suggesting the presence of only one type of phosphorus center in the solution state. In the solid-state cross-polarization magic-angle spinning (CP-MAS) ³¹P{¹H} NMR spectrum, this resonance is only slightly shifted to δ = −4.3 ppm.

With the confirmation of the crucial H-bonding interaction of C2–H of the imidazolium cation with anionic phosphate monoesters at hand, we considered the use of the 2-methylimidazolium cation instead, in which the C2 position is blocked from H-bonding by a methyl substituent. Accordingly, a 1:1 reaction of **3** with 2-methylimidazole in CH₃CN resulted in a white precipitate, and suitable single

Scheme 4. Synthesis of 10

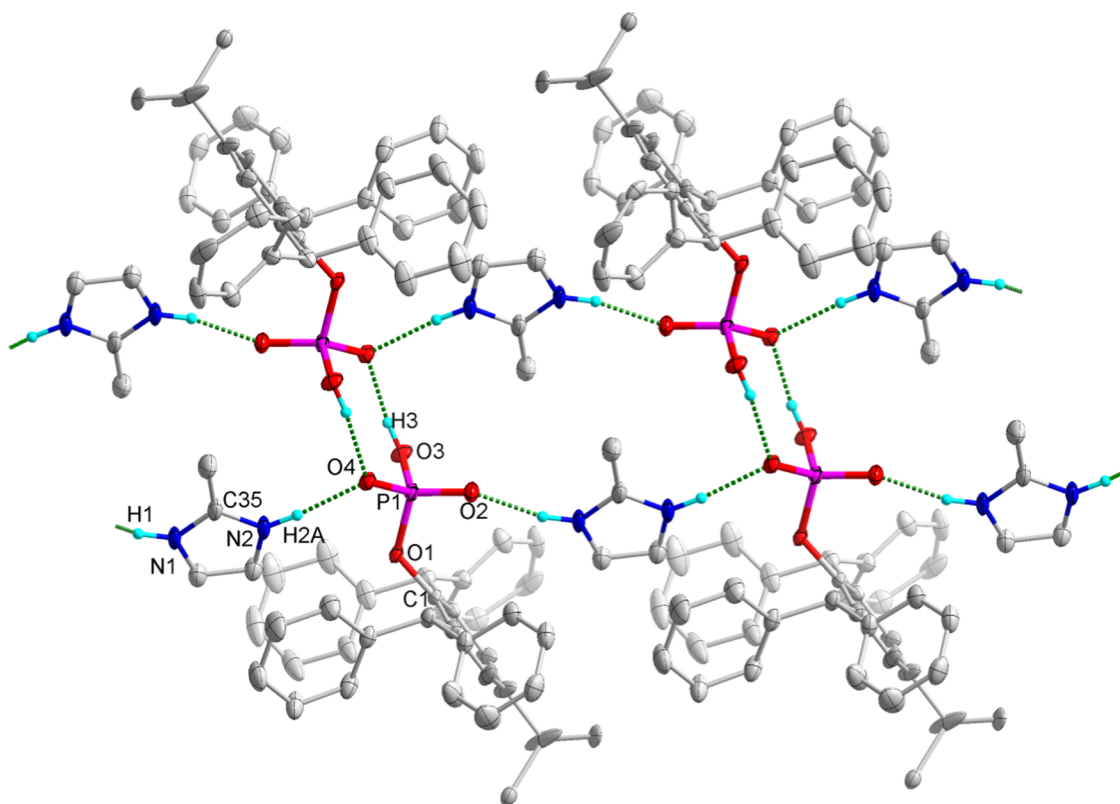
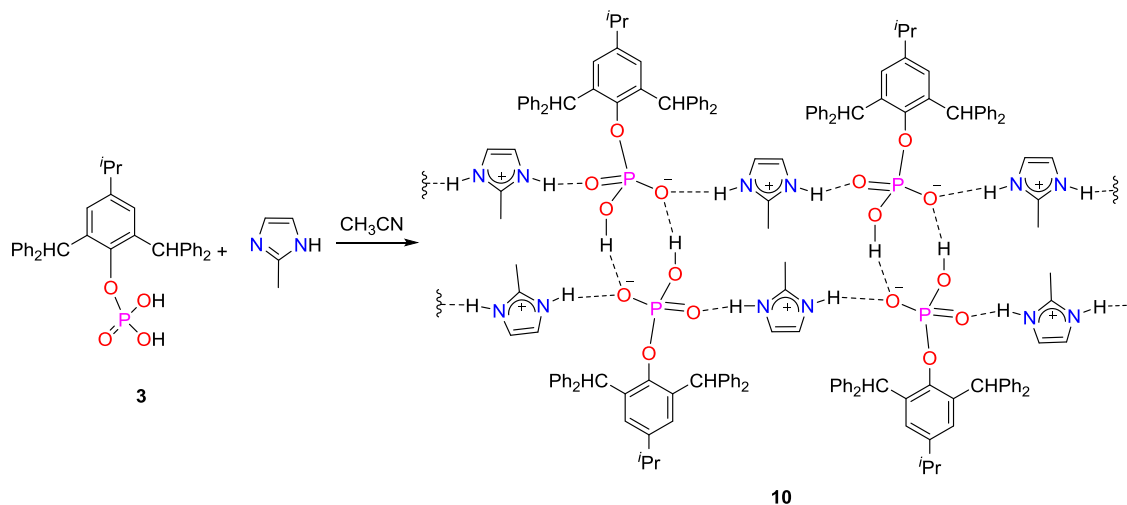


Figure 2. Hydrogen-bonding structure of **10** with thermal ellipsoids of 30% probability. Selected bond lengths (Å) and bond angles (deg): P(1)–O(4) 1.5070(2), P(1)–O(2) 1.4860(2), P(1)–O(4) 1.5705(2), O(4)–P(1)–O(1) 105.00(9), O(4)–P(1)–O(3) 109.65(9), O(2)–P(1)–O(1) 109.33(9), O(2)–P(1)–O(4) 118.17(1), O(2)–P(1)–O(3) 111.99(1), O(3)–P(1)–O(1) 101.08(9). Selected H-bond distances (Å) and angles (deg): O(3)⋯O(4)* 2.6447(2), H(3)⋯O(4)* 1.8088(2), O(3)–H(3)⋯O(4)* 173.162(1), N(1)⋯O(2) 2.6771(3), H(1)⋯O(2) 1.8105(3), N(1)–H(1)⋯O(2) 167.968(2), N(2)⋯O(4) 2.8096(3), H(2A)⋯O(4) 1.9326(2), N(2)–H(2A)⋯O(4) 174.849(2). (*1 – *x*, 1 – *y*, 1 – *z*).

crystals of **10** were obtained from its saturated solution in a DMF/CH₃OH mixture (Scheme 4).

The solid-state molecular structure of **10** reveals that a 1D polymer is formed through the H-bonding interaction of two N–H units of the 2-methylimidazolium cation with the P=O moieties of two adjacent phosphate units (Figure 2). The two polymeric strands are interconnected through O–H⋯O hydrogen bonding between two phosphate moieties, resulting in a double-lane, rail-road architecture. The hydrogen bonding between the two phosphate motifs leads to the formation of an

eight-membered P₂O₄H₂ ring similar to what had been observed in the ion pair with the triethylammonium cation.²⁶ The solution- and solid-state CP-MAS ³¹P{¹H} NMR spectra of **10** shows single singlet resonances at δ = –4.6 and –3.9 ppm, respectively, suggesting the presence of only one type of phosphorus center in the molecule.

After having received different H-bonded structures of anionic phosphate monoesters with imidazolium and 2-methylimidazolium cations, the next logical step was to employ the *N*-methylimidazolium cation in which one of the N–H

Scheme 5. Synthesis of 11

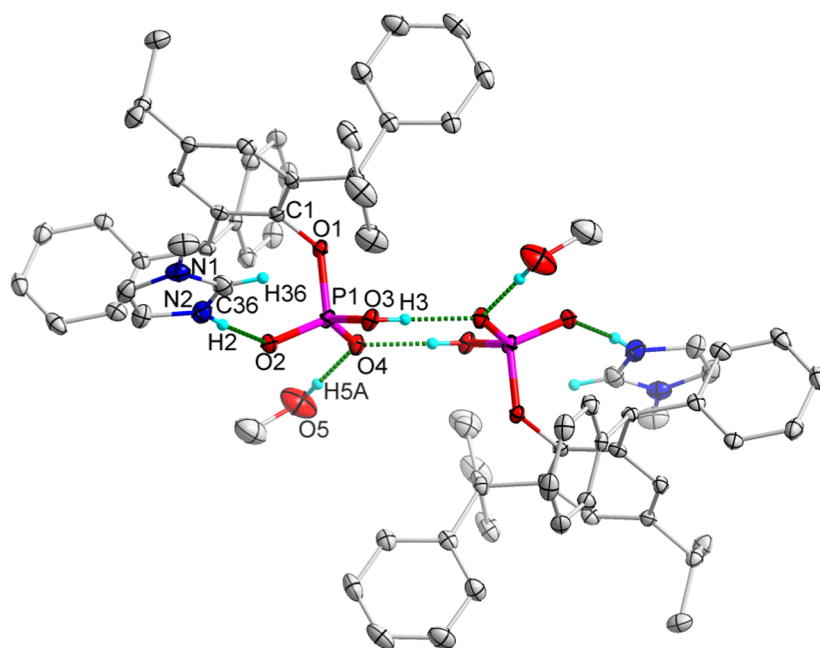
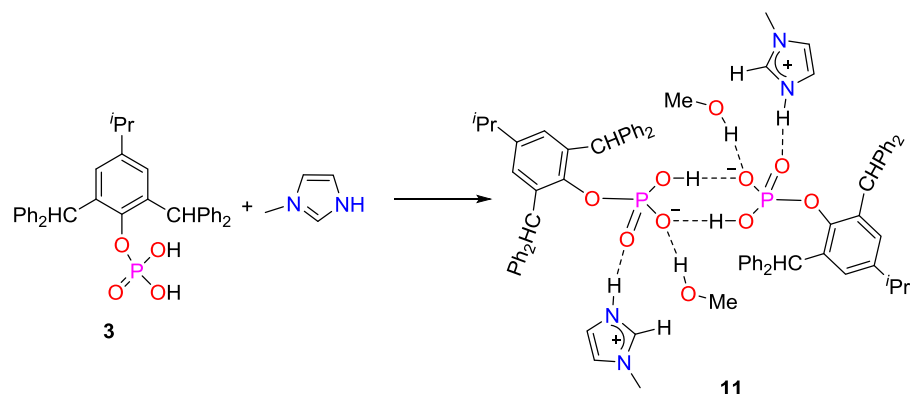
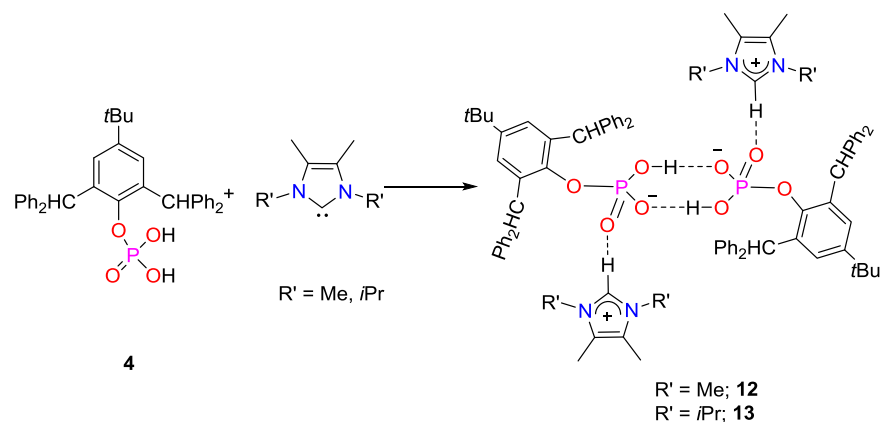


Figure 3. Hydrogen-bonding structure of 11 with thermal ellipsoids of 30% probability. Selected bond lengths (Å) and bond angles (deg): P(1)–O(2) 1.490(1), P(1)–O(3) 1.563(1), P(1)–O(4) 1.499(1), O(2)–P(1)–O(3) 108.51(5), O(2)–P(1)–O(4) 117.46(6), O(4)–P(1)–O(3) 111.24(5). Selected H-bond distances (Å) and angles (deg): O(3)⋯O(4)* 2.543(2), H(3)⋯O(4)* 1.729(1), O(3)–H(3)⋯O(4)* 171.42(7), N(2)⋯O(2) 2.629(2), H(2)⋯O(2) 1.772(1), N(2)–H(2)⋯O(2) 174.330(9), O(5)⋯O(4) 2.779(2), H(5A)⋯O(4) 1.965(9), O(5)–H(5A)⋯O(4) 171.67(9). (*1 – x, 1 – y, 1 – z).

Scheme 6. Syntheses of 12 and 13



sites is replaced by an *N*-methyl moiety. Would it still function as a mixed *N*–H/*C*–H donor or merely as an *N*–H donor? A

1:1 reaction of 3 with *N*-methyl imidazole in CH_3CN afforded a white solid that was crystallized from a saturated MeOH

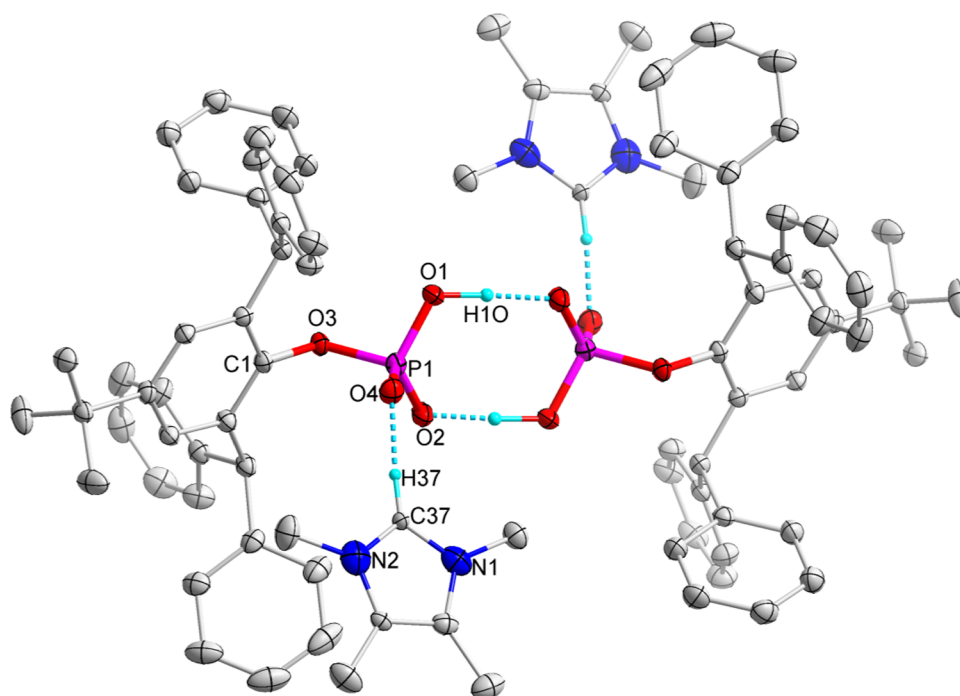


Figure 4. Hydrogen-bonding structure of **12** with thermal ellipsoids of 30% probability. Selected bond lengths (Å) and bond angles (deg): P(1)–O(4) 1.486(2), P(1)–O(2) 1.506(2), P(1)–O(1) 1.538(2), P(1)–O(3) 1.614(2), O(4)–P(1)–O(2) 115.52(14), O(4)–P(1)–O(1) 112.78(1), O(2)–P(1)–O(1) 111.65(1), O(4)–P(1)–O(3) 107.71(1), O(2)–P(1)–O(3) 106.08(1), O(1)–P(1)–O(3) 101.85(1), O(1)···O(2)* 2.5189(1), H(10)···O(2)* 1.4290(1), O(1)–H(10)···O(2)* 169.185(3), O(4)···C(37) 2.600(1), H(37)···O(4) 1.655(1), C(37)–H(37)···O(4) 172.94(4), C(37)–H(37) 0.950. (*1 – *x*, 2 – *y*, 1 – *z*).

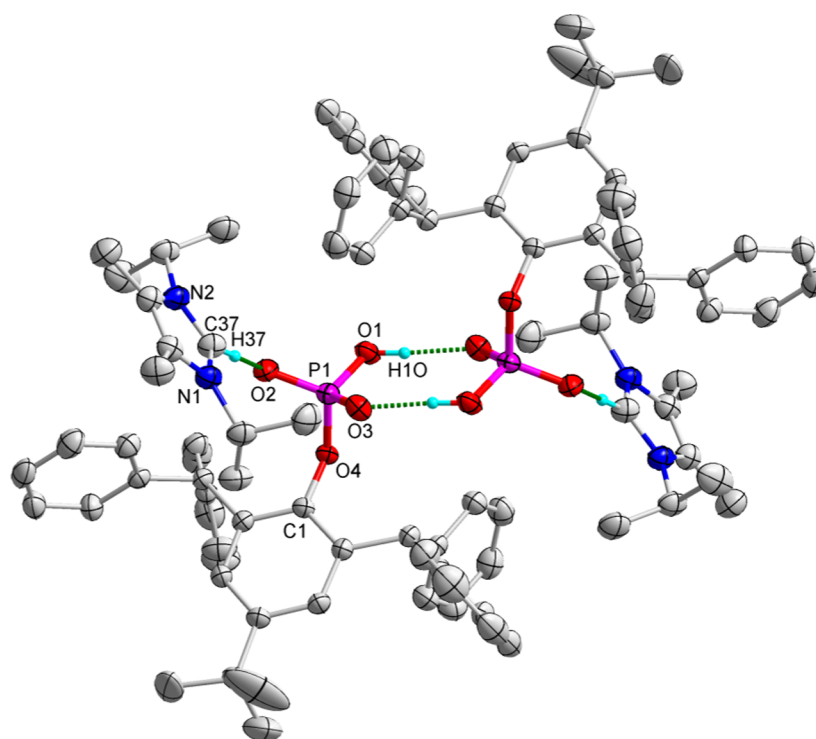


Figure 5. Hydrogen-bonding structure of **13** with thermal ellipsoids of 30% probability. Selected bond lengths (Å) and bond angles (deg): P(1)–O(2) 1.480(1), P(1)–O(3) 1.498(1), P(1)–O(1) 1.554(1), P(1)–O(4) 1.635(1), O(2)–P(1)–O(3) 116.00(7), O(2)–P(1)–O(1) 111.21(7), O(3)–P(1)–O(1) 111.76(7), O(2)–P(1)–O(4) 108.37(7), O(3)–P(1)–O(4) 108.82(6), O(1)–P(1)–O(4) 99.27(6), O(1)···O(3)* 2.545(7), H(10)···O(3)* 1.697(5), O(1)–H(10)···O(3)* 175.48(2), O(2)···C(37) 3.003(6), H(37)···O(2) 2.099(4), C(37)–H(37)···O(2) 164.07(5), C(37)–H(37) 0.929(2). (*2 – *x*, 1 – *y*, 1 – *z*).

solution to afford X-ray quality crystals of **11** in good yield (Scheme 5).

Analysis of the solid-state structure of **11** reveals that it possesses a discrete eight-membered P₂O₄H₂ core with

Scheme 7. Synthesis of 14

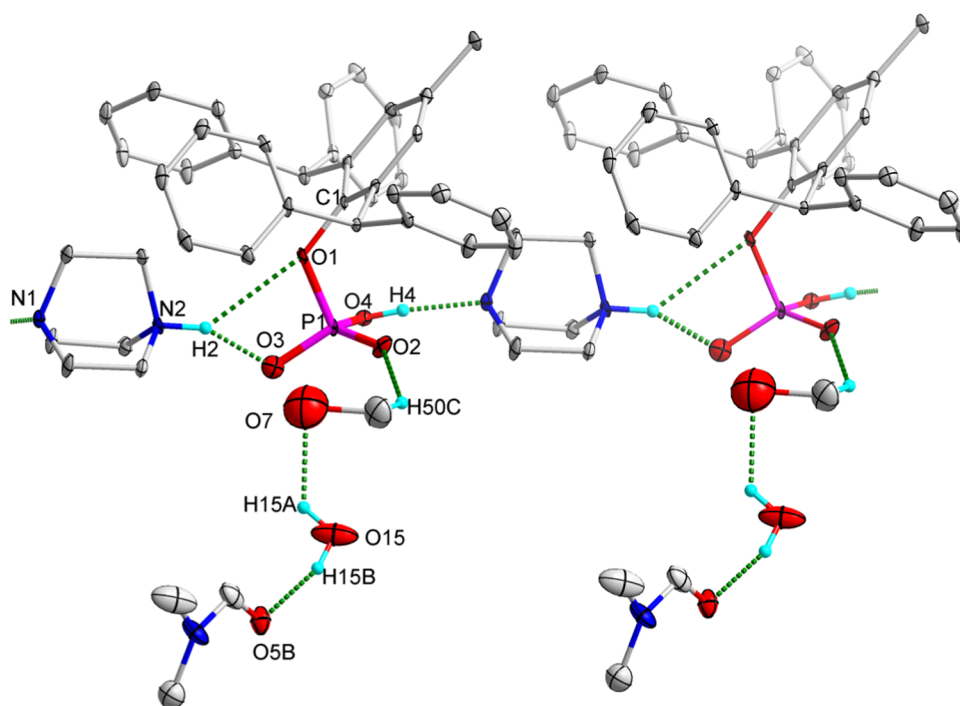
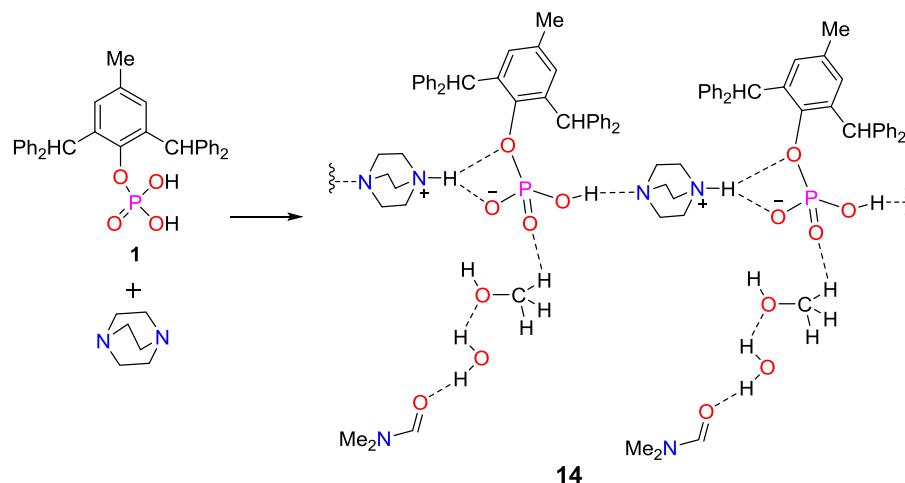


Figure 6. Hydrogen-bonding structure of 14 with thermal ellipsoids of 30% probability.

intermolecular O–H···O hydrogen bonds between two anionic phosphate units similar to the motif observed in the case of **10**. The counter cation is relegated to a supporting role with weak hydrogen-bonding interaction found between the *N*-methylimidazolium N–H and a P=O moiety with an O···H distance of 1.772(1) Å (D···A distance 2.629(2) Å). CH₃OH as solvent used for crystallization is also involved in a H-bonding interaction with the P–O moiety with an O···H distance of 1.965(9) Å (D···A distance 2.779(1) Å) (Figure 3). The ³¹P{¹H} solution NMR spectra of **11** reveal the presence of a singlet at $\delta = -3.3$ ppm.

Next, we considered doubly *N*-alkylated *N,N'*-dialkylimidazolium cations to fully suppress the NH hydrogen-bonding capability only leaving C2–H as possible H-bonding donor.^{28,29} *N,N'*-Dialkylimidazolium cations are readily available from *N,N'*-dialkylimidazol-2-ylidenes (NHC) as precursors.³⁰ NHCs as strong Lewis bases are readily

protonated to imidazolium cations.³¹ In this study, we employed 1,3,4,5-tetramethylimidazol-2-ylidene, NHC^{Me₄},³² and 1,3-diisopropyl-4,5-dimethylimidazol-2-ylidene, NHC^{iPr₂Me₂},³² as precursors to *N,N'*-dialkylimidazolium counter cations with differing steric bulk at the *N* centers to directly deprotonate anionic phosphate monoesters.³³ Indeed, the 1:1 reactions of **4** with NHC^{Me₄} and NHC^{iPr₂Me₂} in dry tetrahydrofuran (THF) afforded compounds **12** and **13**, respectively (Scheme 6). These were crystallized from saturated acetonitrile solutions at 0 °C.

Analysis of the solid-state molecular structures of **12** and **13** reveals that both compounds possess a discrete eight-membered P₂O₄H₂ core through intermolecular O–H···O hydrogen bonds. Importantly, a weak hydrogen-bonding interaction was also found between the imidazolium C–H hydrogen and the P=O moiety of phosphate with the C–H···O distance 3.003(6) Å in **13** compared to 2.600(1) Å in **12**.

Scheme 8. Synthesis of 15

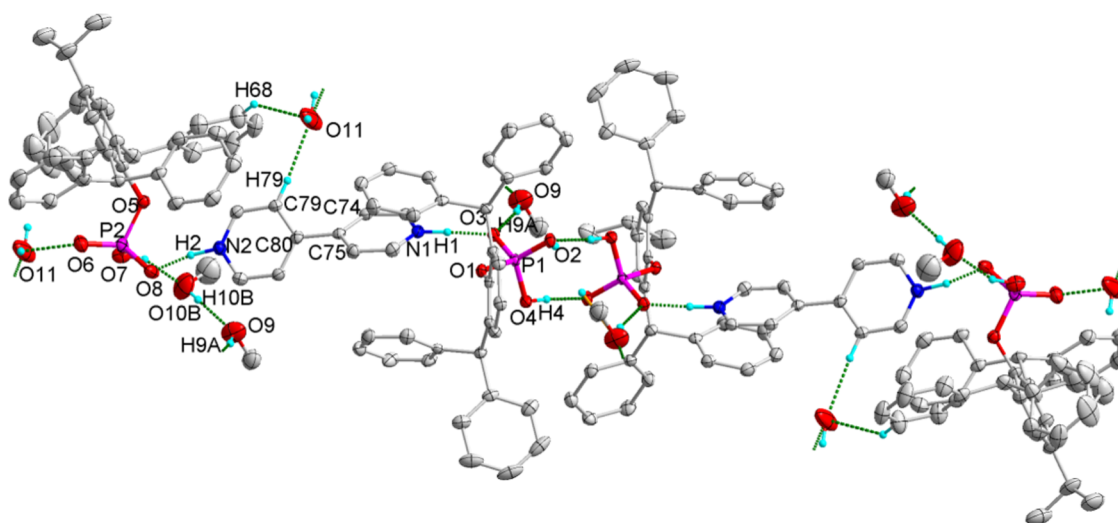
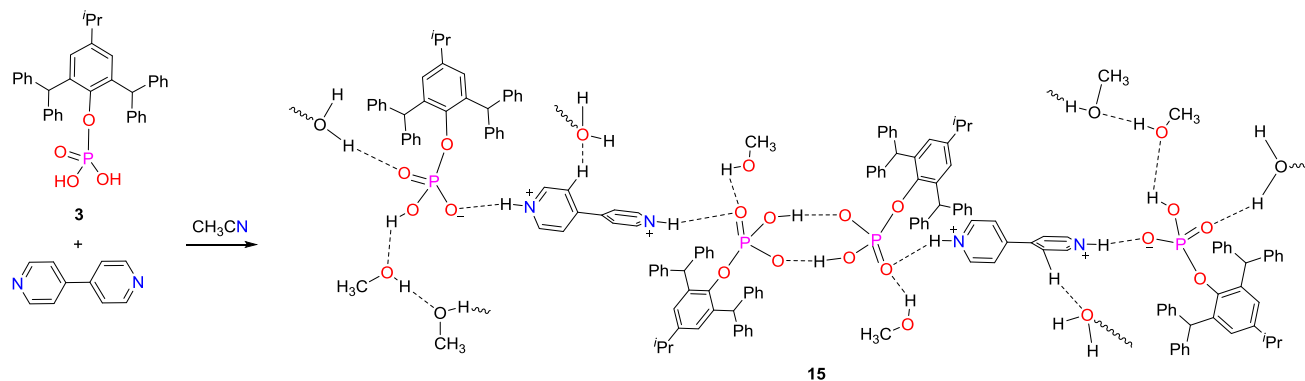


Figure 7. H-bonding structure of 15 with thermal ellipsoids of 30% probability. Selected bond lengths (Å) and bond angles (deg): P(1)–O(2) 1.472(3), P(1)–O(4) 1.490(3), P(1)–O(3) 1.566(3), P(1)–O(1) 1.621(3), P(2)–O(8) 1.493(3), P(2)–O(6) 1.497(3), P(2)–O(7) 1.561(3), P(2)–O(5) 1.605(3), O(2)–P(1)–O(4) 118.4(2), O(2)–P(1)–O(3) 108.0(2), O(4)–P(1)–O(3) 109.06(2), O(2)–P(1)–O(1) 112.26(2), O(4)–P(1)–O(1) 102.82(2), O(3)–P(1)–O(1) 105.55(2), O(8)–P(2)–O(6) 115.42(2), O(8)–P(2)–O(7) 111.20(2), O(6)–P(2)–O(7) 111.21(2), O(8)–P(2)–O(5) 109.89(2), O(6)–P(2)–O(5) 104.04(2), O(7)–P(2)–O(5) 104.23(2), O(8)⋯O(7)* 2.525(8), H(8A)⋯O(7)* 2.090(6), O(8)–H(8A)⋯O(7)* 111.77(5), O(6)⋯N(2) 2.590(7), H(2)N⋯O(6) 1.595(5), N(2)–H(2)N⋯O(6) 173.37(6), O(6)⋯O(10) 2.750(8), H(10A)⋯O(6) 1.912(5), O(10)–H(10A)⋯O(6) 175.07(4), O(4)⋯N(1) 2.495(5), H(1)N⋯O(4) 1.341(3), N(1)–H(1)N⋯O(4) 169.35(6), O(2)⋯O(11) 2.439(6), H(11)⋯O(2) 1.878(4), O(11)–H(11)⋯O(2) 122.98(5), O(3)⋯O(9) 2.739(8), H(3A)⋯O(9) 1.934(6), O(3)–H(3A)⋯O(9) 160.30(7). (*2 – *x*, –*y*, 1 – *z*).

The smaller distance in the case of **12** is readily explained by the less sterically encumbered CH hydrogen-bond donor. The imidazolium C–H bond lengths were determined to be 0.950 and 0.929(2) Å for **12** and **13**, respectively, which is slightly elongated compared to imidazolium salts not involved in any H-bonding with the counter anion, e.g., [NHC^{Dip}H][B(C₆F₅)₃Cl] (0.88(2) Å) (NHC^{Dip} = 1,3-bis(2,6-diisopropylphenyl)imidazol-2-ylidene)³⁴ (Figures 4 and 5).

In the ¹H NMR spectra, downfield resonances at δ = 9.29 and 9.89 ppm were detected for the imidazolium C2–H for **12** and **13**, respectively. In the ¹³C{¹H} NMR spectra, the resonances at δ = 137.1 and 136.0 ppm are assigned to the C2 carbon of the imidazolium moiety of **12** and **13**, respectively. These signals are considerably upfield-shifted compared to those of the corresponding NHC.¹¹ The solution- and solid-state (CP-MAS) ³¹P{¹H} NMR spectra of **12** and **13** show a single singlet resonance at δ = –2.3 and –3.0 ppm and δ = –4.9 and –3.4 ppm, respectively.

After the imidazolium-based cations, which contain only H-bond donor unit(s), we considered 1,4-diazabicyclo[2.2.2]-

octane (DABCO), which should result in the 1,4-diazabicyclo[2.2.2]octan-1-ium cation **VII** with both H-bond acceptor and H-bond donor sites and thus capable of functioning in a ditopic manner.^{35–37} Compound **14** was obtained by treating the ligand **1** with 1 equiv of DABCO and crystallized from a hot DMF/CH₃OH mixture (Scheme 7). So far, we were unable to obtain high-quality single-crystal X-ray diffraction data, and therefore, we are not discussing any metric parameters of this compound (Figure 6).

After considering the ion pairs of anionic phosphate monoesters with different monocations, we investigated the syntheses of ion pairs of anionic phosphate monoesters with dications. Initially, we turned our attention to the *N,N'*-dihydro-4,4'-bipyridinium dication **VIII**. Thus, **15** was synthesized from **3** and 4,4'-bipyridine in a 2:1 ratio. The resulting solid was crystallized from CH₃OH (Scheme 8). The product **15** contained a bis-protonated 4,4'-bipyridyl motif, which served to neutralize the charge of two phosphate anions.

Crystal structure analysis of **15** reveals a one-dimensional polymer with two distinct phosphate motifs (Scheme 8). The

Scheme 9. Syntheses of 16 and 17

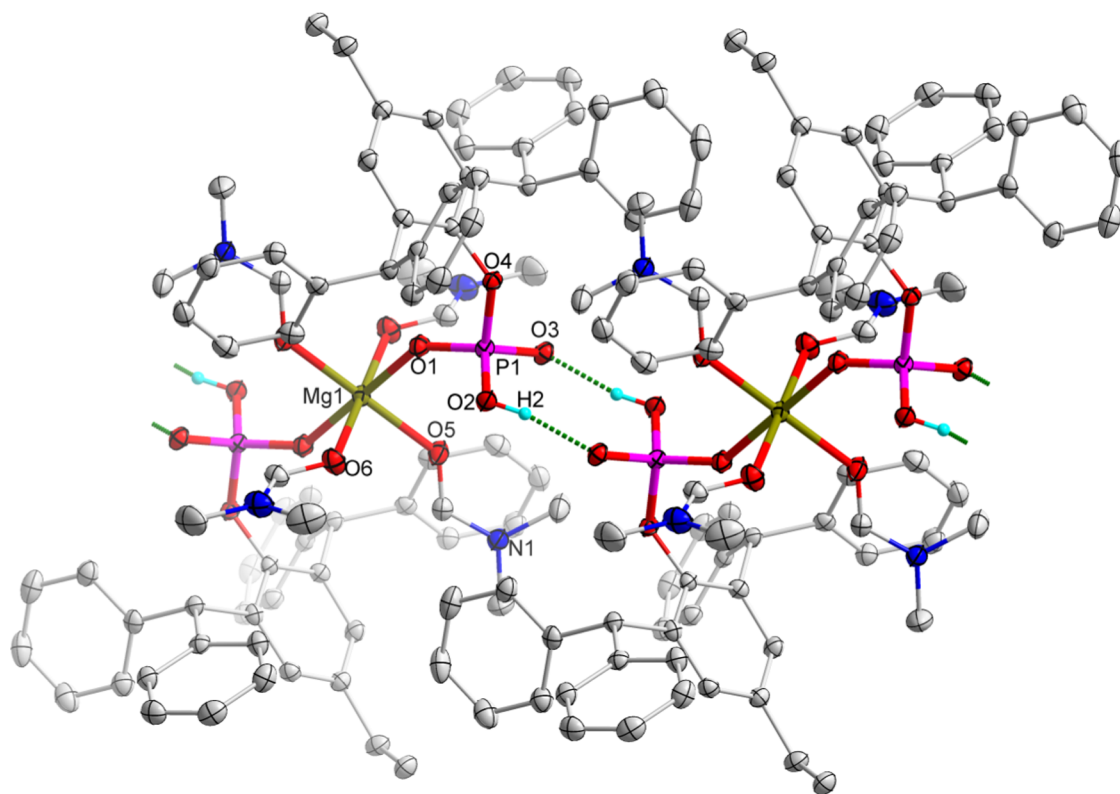
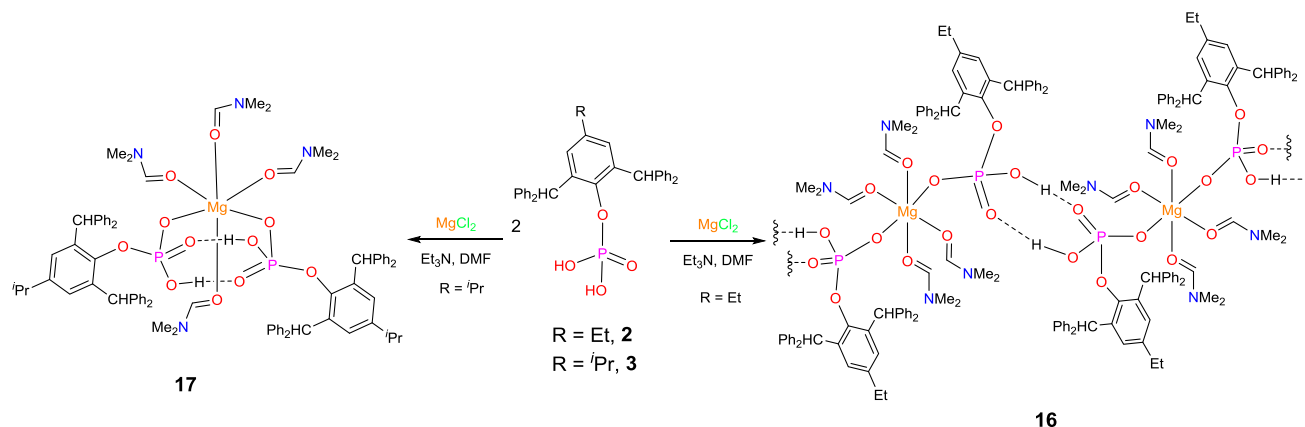


Figure 8. H-bonding structure of **16** with thermal ellipsoids of 50% probability. Selected bond lengths (Å) and bond angles (deg): Mg(1)–O(1) 2.062(9), Mg(1)–O(5) 2.030(9), Mg(1)–O(6) 2.092(1), P(1)–O(1) 1.489(10), P(1)–O(2) 1.564(9), P(1)–O(3) 1.497(9), P(1)–O(4) 1.636(9), O(1)–Mg(1)–O(1)* 180.0, O(1)–Mg(1)–O(6) 90.87(4), O(1)*–Mg(1)–O(6) 89.13(4), O(5)*–Mg(1)–O(1)* 89.30(4), O(5)–Mg(1)–O(1)* 90.70(4), O(5)–Mg(1)–O(1) 89.29(4), O(5)–Mg(1)–O(5)* 180.0, O(5)–Mg(1)–O(6)* 89.64(4), O(5)–Mg(1)–O(6) 90.36(4), O(6)*–Mg(1)–O(6) 180.0, O(1)–P(1)–O(2) 110.68(5), O(1)–P(1)–O(3) 118.78(5), O(1)–P(1)–O(4) 106.70(5), O(2)–P(1)–O(4) 101.55(5), O(3)–P(1)–O(2) 110.97(5), O(3)–P(1)–O(4) 106.54(5), P(1)–O(1)–Mg(1) 141.83(6), O(2)⋯O(3)* 2.609(1), H(2)⋯O(3)* 1.784(9), O(2)–H(2)⋯O(3)* 166.65(7). (O(1)* – $x, 1 - y, 1 - z$), (O(3)* 1 – $x, 1 - y, 1 - z$), (O(5)* – $x, 1 - y, 1 - z$), (O(6)* – $x, 1 - y, 1 - z$).

CP-MAS of $^{31}\text{P}\{^1\text{H}\}$ NMR spectrum reveals the presence of three signals at $\delta = -1.3, -4.3,$ and -5.2 ppm. In contrast, the $^{31}\text{P}\{^1\text{H}\}$ NMR spectra of this compound in CDCl_3 with a small amount of DMF exhibit only one singlet at $\delta = -4.2$ ppm, suggesting that the solid-state structure is not retained in solution. The crystal structure of **15** reveals that both monomeric and dimeric phosphate units are present in a chain connected to each other through the bipyridinium cation. The P=O of the dimeric motif is simultaneously H-bonded to the N–H of the bridging bipyridinium cation and a

molecule of methanol. The second bipyridinium N–H is involved in polymer propagation through its interaction with a P–O unit of a monomeric phosphate motif. The P–OH of the latter is tied down by the interaction with another solvent molecule (MeOH). The two pyridyl rings of the 4,4'-bipyridine motif are twisted by a torsional angle of $44.206(76)^\circ$ (Figure 7).

So far, all of the mono- and dications discussed have the potential to be involved in H-bonding interactions, as shown above. Finally, we were interested in a cation, which can only

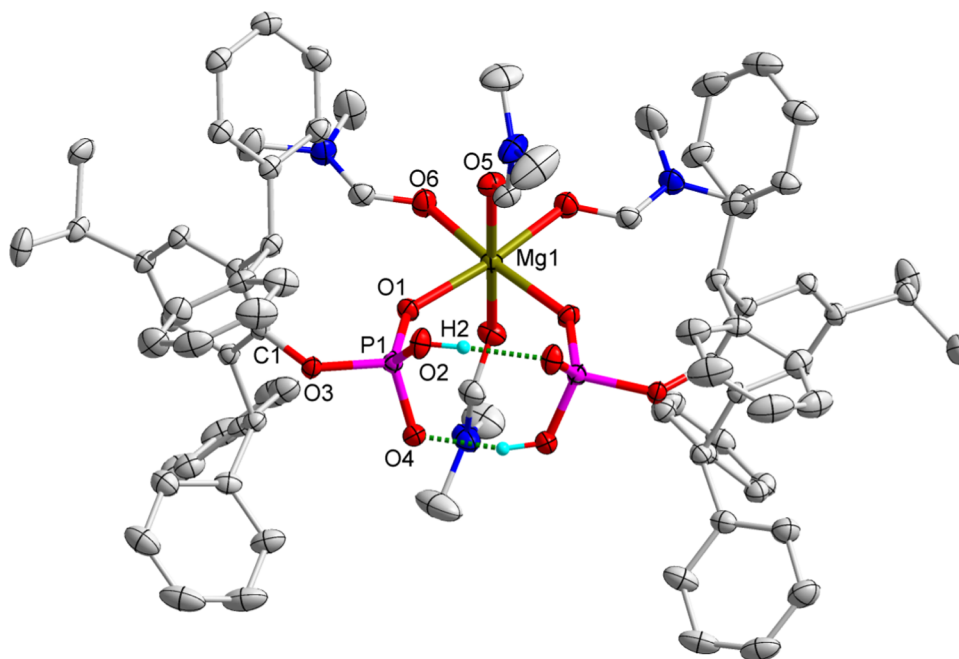


Figure 9. H-bonded molecular structure of **17** with thermal ellipsoids of 50% probability. Selected bond lengths (Å) and bond angles (deg): Mg(1)–O(6) 2.060(2), Mg(1)–O(1) 2.082(2), Mg(1)–O(5) 2.130(2), P(1)–O(1) 1.491(2), P(1)–O(4) 1.523(2), P(1)–O(2) 1.535(2), P(1)–O(3) 1.605(2), O(6)–Mg(1)–O(6)* 84.52(1), O(6)–Mg(1)–O(1)* 89.04(7), O(6)–Mg(1)–O(1) 173.35(8), O(6)*–Mg(1)–O(1) 89.03(7), O(1)*–Mg(1)–O(1) 97.46(1), O(6)–Mg(1)–O(5)* 87.60(8), O(1)–Mg(1)–O(5)* 90.75(7), O(6)–Mg(1)–O(5) 89.64(8), O(1)*–Mg(1)–O(5) 90.75(7), O(1)–Mg(1)–O(5) 91.71(7), O(5)*–Mg(1)–O(5) 176.28(1), O(1)–P(1)–O(4) 114.18(1), O(1)–P(1)–O(2) 113.76(1), O(4)–P(1)–O(2) 110.37(1), O(1)–P(1)–O(3) 110.07(9), O(4)–P(1)–O(3) 104.01(9), O(2)–P(1)–O(3) 103.44(9), O(2)...O(4)* 2.5730(2), H(2)...O(4)* 1.750(7), O(2)–H(2)...O(4)* 163.03(8). (O(1)*1 - x, y, 0.5 - z), (O(5)*1 - x, y, 0.5 - z), (O(6)*1 - x, y, 0.5 - z), (O(4)*1 - x, y, 0.5 - z).

serve to neutralize the charge of the phosphate anions, but will not have the capability to be involved in a hydrogen-bonding interaction. The magnesium(II) dication **IX** was chosen as the coordination of phosphate monoesters and diesters with magnesium salts has been studied previously.^{38,39} The reaction of 2 equiv of **2** and **3** with anhydrous MgCl_2 in the presence of Et_3N resulted in a precipitate that was crystallized from either DMF or DMF/ CH_3CN mixture affording magnesium metallophosphates **16** and **17**, respectively (Scheme 9).

Surprisingly, the molecular structures in the solid state are different with the variation of the aryl para substituents of the phosphate monoesters from -Et to -ⁱPr. The solid-state molecular structure of **16** reveals the formation of a 1D polymeric chain through intermolecular H-bonding between the phosphate moieties to an eight-membered $\text{P}_2\text{O}_4\text{H}_2$ core and the coordination of P–O to the octahedral Mg(II) center in a trans manner (Figure 8). The other four coordination sites of the magnesium centers are occupied by DMF.

On the other hand, the molecular structure of **17** reveals a discrete magnesium metallophosphate, where the coordination of P–O to the octahedral Mg(II) center occurs in a cis manner enabling the formation of the eight-membered $\text{P}_2\text{O}_4\text{H}_2$ H-bonded core through intramolecular H-bonding interaction of two anionic phosphate moieties (Figure 9). Here, as well, the remaining four coordination sites of the Mg(II) center are occupied by four DMF molecules.

Compounds **16** and **17** can formally be considered as regioisomers (cis/trans) with respect to the coordination of P–O to the Mg(II) center. In the case of the trans geometry, the 1D polymeric network of magnesium phosphate is formed, while for the cis geometry, only the discrete magnesium

phosphate is obtained. The solution-state $^{31}\text{P}\{^1\text{H}\}$ NMR spectra of **16** and **17** reveal the presence of multiple singlet resonances in both cases ($\delta = -4.9, -6.1, -8.2, -8.7,$ and -10.4 ppm for **16** and $\delta = -4.9, -6.2, -8.4, -8.7,$ and -10.4 ppm for **17**), which could be due to the fact that in solution, these Mg phosphate complexes exist in more than one form. The solid-state $^{31}\text{P}\{^1\text{H}\}$ NMR spectrum of **16** reveals the presence of a single resonance at $\delta = -5.6$ ppm, whereas **17** exhibits two resonances at $\delta = -0.5$ and -8.8 ppm. The resonance at $\delta = -0.5$ ppm is considerably lower in intensity compared to the resonance at $\delta = -8.8$ ppm, which might be due to the exchange of DMF with water during the sample preparation. We repeatedly measured various single crystals of **16** and **17** to ascertain whether other structural forms were present. However, we were unable to detect any structures different from the ones discussed above. It is likely that the solid-state structures of **16** and **17** correspond to the thermodynamically stable forms, although this cannot be asserted with certainty.

For all newly synthesized compounds, Fourier transform infrared spectra were recorded; the presence of broad absorption bands around 2491, 2430, 2389, 2386, 2408, 2423, 2389, 2390, and 2392 cm^{-1} and sharp absorption bands appearing at 1176, 1189, 1161, 1190, 1187, 1177, 1160, 1203, and 1161 cm^{-1} correspond to a P–OH and P=O group of **9**, **10**, **11**, **12**, **13**, **14**, **15**, **16**, and **17**, respectively.²⁶ The imidazolium C–H stretching frequencies of compounds **9**, **10**, **11**, **12**, and **13** appear at 3140, 3139, 3138, 3173, and 3152 cm^{-1} , respectively.^{40,41} We have also performed the Hirshfeld surface calculations of all of these newly synthesized

compounds to gain more insight into noncovalent interaction (see the Supporting Information for details).

3. CONCLUSIONS

The structure of the ion pairs of the phosphate monoesters strongly depends on the nature of the counter cations employed. Among the imidazolium family, *N,N'*-dialkylimidazolium and *N*-methylimidazolium cations lead to a discrete dimer, with the formation of eight-membered $P_2O_4H_2$ H-bonded core, which has been observed previously with triethylammonium cations. On the other hand, imidazolium and 2-methylimidazolium cations afford 1D polymers containing alternate phosphate and cation moieties. In the case of the 2-methylimidazolium cation, a double-lane, rail-road polymer was obtained, in which the two lanes are interconnected by the eight-membered $P_2O_4H_2$ H-bonded ring. An interesting aspect of the crystal structures with imidazolium cations is that the participation of NH and CH units in H-bonding is modulated by the variation in the substituent of the imidazolium units. DABCO as monocation and 4,4'-bipyridine as dication were assembled into polymeric structures, where the former employed both *N*-H donor and *N*-acceptor sites for the interactions. Unsurprisingly, Mg^{2+} only served to neutralize the charge of anionic phosphate monoesters and was not involved in H-bonding. Depending on the mode of phosphate coordination (*cis/trans*) to the Mg center, it forms either a discrete or 1D polymeric structure, both of which contain the eight-membered $P_2O_4H_2$ dimeric motif. In most of the structures examined, the robustness of the dimeric $P_2O_4H_2$ motif is clearly demonstrated, indicating a similar dominance among phosphates as it is well known in the case of carboxylic acids.

4. EXPERIMENTAL SECTION

4.1. General Experimental Considerations. **4.1.1. Materials.** All of the bulky aryl-substituted phosphate monoesters, **1–4**, were synthesized according to the reported procedure.²⁶ Imidazole and *N*-methyl imidazole were obtained from Sigma-Aldrich (Merck), 2-methyl imidazole was obtained from Avra Synthesis Pvt. Ltd., and DABCO and 4,4'-bipyridine were obtained from Alfa Aesar (Thermo Fisher Scientific). NHC^{Me_4} and $NHC^{iPr_2Me_2}$ were synthesized according to the reported procedures.³² Compounds **12** and **13** were synthesized under an argon atmosphere using standard Schlenk techniques, and all remaining reactions were carried out under ambient atmosphere inside a fume hood. THF was dried by an Innovative Technology solvent purification system. $CDCl_3$ was dried and distilled over CaH_2 under argon.

4.1.2. Instrumentation. NMR spectra were recorded on a Bruker NanoBay 300 MHz NMR spectrometer. 1H and $^{13}C\{^1H\}$ NMR spectra were referenced to the peaks of residual protons of the deuterated solvent (1H) or the deuterated solvent itself (^{13}C). $^{31}P\{^1H\}$ NMR spectra were referenced to external H_3PO_4 . IR spectra were recorded on a Bruker- α spectrometer. Melting points were recorded in a Stuart SMP10 melting point apparatus. Elemental analyses of the compounds **9**, **10**, **11**, **14**, **15**, **16**, and **17** were obtained from Thermoquest CE Instruments CHNS-O, EA/1110 model, and PerkinElmer series-II 2400 elemental analyzer. Elemental analyses of compounds **12** and **13** were performed on a LECO CHN-900 analyzer. Electrospray ionization mass spectrometry (ESI-MS) was carried out on a Micromass Quattro II triple

quadrupole mass spectrometer. Solid-state $^{31}P\{^1H\}$ NMR spectra were obtained on a Bruker Avance 400 MHz spectrometer with a wide-bore magnet operating at 400.13 MHz (1H) and 163.32 MHz (^{31}P). Powdered samples were packed in a 4 mm outside diameter zirconia rotor. The diameter of the probe is 89 mm with a spinning speed of 13 kHz. The $^{31}P\{^1H\}$ CP-MAS experiment was performed using a 1H 90° pulse of 3.3 μs , with a contact time of 5 ms, CPD Spinal64 as the decoupling scheme, and a recycle delay of 3 s.

4.2. Synthetic Procedure. **4.2.1. Synthesis of 9.** Imidazole (0.04 g, 0.6 mmol) was added to a clear solution of **4** (0.38 g, 0.6 mmol) in acetonitrile (50 mL) at room temperature and stirred for 20 h. A colorless precipitate was collected by filtering the reaction mixture and crystallized from a DMF and CH_3OH mixture at room temperature to obtain pure crystals of **9** suitable for single-crystal X-ray diffraction analysis. Yield: 0.32 g, 76%. m.p.: 268 °C. 1H NMR ($CDCl_3$ + 0.1 mL DMF, 25 °C): δ = 7.77 (s, 14H), 7.46 (s, DMF), 7.13 (s, 11H), 6.94 (br, 1H), 6.64 (m, 10H), 6.55 (m, 11H), 6.26 (s, 2H), 5.92 (s, 2H), 3.14 (br, 45H), 2.66 (s, 47H), 2.53 (s, 66H), 2.43 (s, DMF), 2.31 (s, DMF), 2.20 (s, 53H), 2.07 (s, 39H), 0.48 (s, 9H) ppm. ^{13}C NMR ($CDCl_3$ + 0.1 mL DMF, 75.431 MHz, 25 °C): 161.8 (DMF), 143.5, 129.0, 127.4, 125.4, 51.1, 45.9, 45.0, 40.0, 38.8, 35.7 (DMF), 35.2, 33.6, 32.7, 30.6 (DMF), 27.5, 26.5, 21.4, 20.4, 15.3 ppm. $^{31}P\{^1H\}$ NMR ($CDCl_3$ + 0.1 mL DMF, 121.442 MHz, 25 °C): δ = -4.7 ppm. CP-MAS $^{31}P\{^1H\}$ NMR (163.32 MHz, 298 K): δ = -4.3 ppm. IR (KBr pellet, cm^{-1}): $\bar{\nu}$ = 3441 (s, br), 3140 (m), 3084 (w), 3061 (w), 3026 (w), 2963 (s), 2865 (w), 2491 (w, br), 1952 (w), 1646 (s), 1599 (m), 1494 (m), 1448 (m), 1414 (w), 1388 (w), 1363 (w), 1294 (w), 1235 (m), 1176 (s), 1100 (s), 1078 (s), 1032 (w), 923 (s), 907 (s), 894 (s), 786 (w), 762 (w), 717 (s), 702 (vs), 665 (w), 633 (w), 605 (w), 589 (w), 566 (w), 547 (w), 532 (w), 505 (w). ESI-MS: calcd (m/z) for $[C_{36}H_{34}O_4P]^-$ 561.2195; found: 561.2194 and calcd (m/z) for $[C_3H_5N_2]^+$ 69.0453; found: 69.0477. Elemental analysis calcd (%) for $C_{42}H_{46}N_3O_5P$: C, 71.67; H, 6.59; N, 5.97; found: C 71.95, H 6.33, N 6.01.

4.2.2. Synthesis of 10. 2-Methyl imidazole (0.05 g, 0.05 mL, 0.6 mmol) was added to a suspension of **3** (0.37 g, 0.6 mmol) in acetonitrile (80 mL) at room temperature and stirred for 72 h. The colorless precipitate was collected by filtering the reaction mixture and recrystallized from a DMF and CH_3OH mixture at room temperature to obtain pure crystals of **10**. Yield: 0.25 g, 69%. m.p.: 258 °C. 1H NMR ($CDCl_3$ + 0.1 mL DMF, 25 °C): δ = 7.94 (s, 13H), 7.62 (br, DMF), 7.28–7.30 (m, 26H, Ar-H), 6.87 (s, 2H), 6.75–6.82 (m, 2H), 6.68–6.73 (m, 3H), 6.25 (s, 1H), 6.07 (s, 1H), 2.6 (s, DMF), 2.46 (s, DMF), 2.36 (s, DMF), 2.24 (s, DMF), 0.60 (d, 6H), ppm. ^{13}C NMR ($CDCl_3$ + 0.1 mL DMF, 75.431 MHz, 25 °C): 162.1 (DMF), 143.6, 129.1, 127.4, 125.5, 121.1, 51.3, 46.2, 45.2, 40.1, 39.0, 36.0 (DMF), 33.9, 32.9, 30.8 (DMF), 27.7, 26.8, 21.6, 20.6, 15.5 ppm. $^{31}P\{^1H\}$ NMR ($CDCl_3$ + 0.1 mL DMF, 121.442 MHz, 25 °C): δ = -4.6 ppm. CP-MAS $^{31}P\{^1H\}$ NMR (163.32 MHz, 298 K): δ = -3.9 ppm. IR (KBr pellet, cm^{-1}): $\bar{\nu}$ = 3441 (s, br), 3163 (w), 3139 (w), 3084 (w), 3026 (w), 2960 (m), 2925 (w), 2867 (w), 2685 (w), 2584 (w), 2430 (w), 1948 (w), 1632 (m), 1600 (w), 1494 (m), 1446 (m), 1384 (w), 1318 (w), 1264 (w), 1240 (w), 1189 (vs), 1119 (w), 1085 (s), 1032 (w), 986 (w), 963 (w), 920 (s), 909 (vs), 866 (w), 853 (w), 829 (w), 799 (w), 756 (w), 714 (s), 699 (vs), 666 (w), 648 (w), 631 (w), 620 (w), 604 (w), 590 (w), 570 (w), 577 (w), 556 (w). ESI-MS: calcd (m/z) for

$[\text{C}_{35}\text{H}_{32}\text{O}_4\text{P}]^-$: 547.2038; found: 547.2036 and calcd (m/z) for $[\text{C}_4\text{H}_7\text{N}_2]^+$: 83.0609; found: 83.0631. Elemental analysis calcd (%) for $\text{C}_{39}\text{H}_{39}\text{N}_2\text{O}_4\text{P}$: C, 74.27; H, 6.23; N, 4.44; found: C 73.32, H 6.14, N 4.60.

4.2.3. Synthesis of 11. *N*-Methyl imidazole (0.05 g, 0.05 mL, 0.6 mmol) was added to a suspension of **3** (0.37 g, 0.6 mmol) in acetonitrile (50 mL) at room temperature and stirred for 72 h. The colorless precipitate was collected by filtering the reaction mixture and recrystallized from a saturated CH_3OH solution at room temperature to obtain pure crystals of **11**. Yield: 0.27 g, 70%. m.p.: 240 °C. ^1H NMR (CDCl_3 , sparingly soluble, 25 °C): δ = 8.15 (s, 1H, $\text{C}-\text{H}_{\text{im}}$), 7.02 (s, br, 16H, $\text{Ar}-\text{H}$), 6.63 (s, br, 2H, $\text{P}-\text{OH}$), 6.38 (s, 2H, CHPh_2), 4.62 (br, 4H), 3.84 (s, CH_3OH), 3.12 (s, CH_3OH), 2.62 (br, 2H, $\text{Ar}-\text{CHMe}_2$), 1.88 (br, DMF), 0.99 (d, 6H, $\text{Ar}-\text{CH}(\text{CH}_3)_2$) ppm. $^{31}\text{P}\{^1\text{H}\}$ NMR (CDCl_3 , 121.442 MHz, 25 °C): δ = -3.3 ppm. CP-MAS $^{31}\text{P}\{^1\text{H}\}$ NMR (163.32 MHz, 298 K): δ = -2.7 and -5.0 ppm. IR (KBr pellet, cm^{-1}): $\bar{\nu}$ = 3424 (w, br), 3138 (w), 3082 (w), 3059 (w), 3025 (w), 2958 (m), 2868 (w), 2389 (w, br), 2344 (w), 1951 (w), 1635 (w), 1599 (m), 1584 (m), 1493 (s), 1467 (m), 1446 (m), 1384 (w), 1280 (m), 1203 (m), 1161 (s), 1125 (s), 1100 (s), 1032 (m), 924 (s), 888 (s), 848 (m), 826 (w), 792 (w), 767 (w), 744 (m), 713 (s), 701 (vs), 660 (w), 647 (w), 630 (w), 606 (w), 592 (w), 577 (w), 561 (w), 533 (w). ESI-MS: calcd (m/z) for $[\text{C}_{35}\text{H}_{32}\text{O}_4\text{P}]^-$: 547.2038; found: 547.2034 and calcd (m/z) for $[\text{C}_4\text{H}_7\text{N}_2]^+$: 83.0609; found: 83.0624. Elemental analysis calcd (%) for $\text{C}_{40}\text{H}_{43}\text{N}_2\text{O}_5\text{P}$: C, 72.49; H, 6.54; N, 4.23; found: C 73.46, H 6.06, N 4.71.

4.2.4. Synthesis of 12. In a 100 mL Schlenk flask, **4** (0.254 g, 0.4 mmol) and NHC^{Me_4} (0.05 g, 0.4 mmol) were combined. Dry THF (30 mL) was added at room temperature and stirred overnight. During this period, a colorless residue was formed and volatiles were removed under vacuum to afford a colorless residue, which was dissolved in a minimum quantity of warm, dry acetonitrile and kept for crystallization at 0 °C to afford suitable single crystals of **12**. Yield: 0.173 g, (63.83%). m.p.: 247 °C. ^1H NMR (300 MHz, CDCl_3 , 298 K): δ = 9.29 (s, 1H, NCHN), 8.07 (br, 1H, $\text{P}-\text{OH}$), 7.12–6.93 (m, 20H, $\text{Ar}-\text{H}$), 6.73 (s, 4H, $\text{Ar}-\text{H} + \text{CHPh}_2$), 2.98 (s, 6H, $\text{N}-\text{CH}_3$), 1.83 (s, 6H, $\text{C}(4,5)-\text{CH}_3$), 0.98 (s, 9H, $\text{C}(\text{CH}_3)_3$) ppm. $^{13}\text{C}\{^1\text{H}\}$ NMR (75.43 MHz, CDCl_3 , 298 K): δ = 145.40 ($\text{Ar}-\text{C}_{\text{quart}}$), 144.45 ($\text{Ar}-\text{C}_{\text{quart}}$), 137.15 ($\text{N}-\text{CH}-\text{N}$), 136.04 ($\text{Ar}-\text{C}_{\text{quart}}$), 129.94 ($\text{Ar}-\text{C}_{\text{quart}}$), 127.36 ($\text{Ar}-\text{CH}$), 125.98 ($\text{Ar}-\text{CH}$), 125.33 [$\text{C}(4,5)$ Im^{Me_4}], 125.03 ($\text{Ar}-\text{CH}$), 49.41 (CHPh_2), 34.13 [$\text{N}(1,3)-(\text{CH}_3)_2$], 32.46 ($\text{C}(\text{CH}_3)_3$), 31.29 ($\text{C}(\text{CH}_3)_3$), 7.96 [$\text{C}(4,5)-\text{CH}_3$] ppm. $^{31}\text{P}\{^1\text{H}\}$ NMR (25 °C, 121.442 MHz, CDCl_3): δ = -2.3 ppm. CP-MAS $^{31}\text{P}\{^1\text{H}\}$ NMR (163.32 MHz, 298 K): δ = -4.9 ppm. IR (KBr pellet, cm^{-1}): $\bar{\nu}$ = 3425 (s, br), 3173 (w), 3112 (w), 3056 (m), 3026 (m), 2958 (s), 2864 (w), 2386 (w), 1641 (m), 1599 (m), 1580 (s), 1493 (s), 1447 (s), 1413 (w), 1392 (w), 1361 (w), 1290 (m), 1271 (m), 1205 (s), 1189 (s), 1100 (s), 1033 (m), 908 (s), 876 (s), 852 (w), 833 (s), 814 (w), 782 (w), 765 (w), 747 (w), 713 (s), 702 (s), 652 (w), 632 (w), 606 (w), 587 (w), 566 (w), 520 (w). ESI-MS: calcd (m/z) for $[\text{C}_{36}\text{H}_{34}\text{O}_4\text{P}]^-$: 561.2195; found: 561.2191 and calcd (m/z) for $[\text{C}_7\text{H}_{13}\text{N}_2]^+$: 125.1079; found: 125.1126. Elemental analysis calcd for $\text{C}_{43}\text{H}_{47}\text{N}_2\text{O}_4\text{P}$ (686.33): C, 75.20; H, 6.90; N, 4.08. Found: C, 74.15; H, 6.33; N, 4.06.

4.2.5. Synthesis of 13. In a 100 mL Schlenk flask, **4** (0.191 g, 0.3 mmol) and $\text{NHC}^{\text{IPr}_2\text{Me}_2}$ (0.054 g, 0.3 mmol) were dissolved in dry THF (20 mL) at room temperature and

stirred overnight. Volatiles were removed under vacuum from the thus formed colorless residue, which was dissolved in a minimum quantity of dry acetonitrile by warming, filtered, and kept for crystallization at 0 °C to afford suitable single crystals of **13**. Yield: 0.126 g, (56.75%). m.p.: 243 °C. ^1H NMR (300 MHz, CDCl_3 , 298 K): δ = 9.89 (s, 1H, NCHN), 7.13–6.97 (m, 20H, $\text{Ar}-\text{H}$), 6.69 (s, 2H, $\text{Ar}-\text{H}$), 6.56 (s, 2H, CHPh_2), 6.49 (br, 1H, $\text{P}-\text{OH}$), 4.18 (sept, 2H, $\text{CH}(\text{CH}_3)_2$), 2.02 (s, 6H, $\text{C}(4,5)-\text{CH}_3$), 1.16 (d, 12H, $\text{CH}(\text{CH}_3)_2$), 1.0 (s, 9H, $\text{C}(\text{CH}_3)_3$) ppm. $^{13}\text{C}\{^1\text{H}\}$ NMR (75.43 MHz, CDCl_3 , 298 K): δ = 145.82 ($\text{Ar}-\text{C}_{\text{quart}}$), 143.59 ($\text{Ar}-\text{C}_{\text{quart}}$), 136.03 ($\text{N}-\text{CH}-\text{N}$), 135.99 ($\text{Ar}-\text{C}_{\text{quart}}$), 135.11 ($\text{Ar}-\text{C}_{\text{quart}}$), 130.13 ($\text{Ar}-\text{C}_{\text{quart}}$), 127.29 ($\text{Ar}-\text{CH}$), 125.75 [$\text{C}(4,5)$ $\text{Im}^{\text{Me}_2\text{IPr}_2}$], 124.99 ($\text{Ar}-\text{CH}$), 124.85 ($\text{Ar}-\text{CH}$), 51.48 (CHPh_2), 49.15 [$\text{N}(1,3)-\text{CH}(\text{CH}_3)_2$], 34.09 ($\text{C}(\text{CH}_3)_3$), 31.37 ($\text{C}(\text{CH}_3)_3$), 21.73 [$\text{N}(1,3)-\text{CH}(\text{CH}_3)_2$], 8.73 [$\text{C}(4,5)-\text{CH}_3$] ppm. $^{31}\text{P}\{^1\text{H}\}$ NMR (25 °C, 121.442 MHz, CDCl_3): δ = -3.0 ppm. CP-MAS $^{31}\text{P}\{^1\text{H}\}$ NMR (163.32 MHz, 298 K): δ = -3.4 ppm. IR (KBr pellet, cm^{-1}): $\bar{\nu}$ = 3425 (m, br), 3058 (w), 3024 (w), 2962 (s), 2408 (w), 1629 (w), 1600 (m), 1550 (m), 1494 (s), 1446 (s), 1393 (w), 1376 (w), 1361 (w), 1248 (m), 1187 (s), 1100 (s), 1032 (m), 914 (s), 880 (s), 853 (w), 832 (w), 784 (w), 765 (m), 746 (w), 651 (w), 631 (w), 606 (w), 588 (w), 569 (w), 549 (w), 524 (w). ESI-MS: calcd (m/z) for $[\text{C}_{36}\text{H}_{34}\text{O}_4\text{P}]^-$: 561.2195; found: 561.2198 and calcd (m/z) for $[\text{C}_{11}\text{H}_{21}\text{N}_2]^+$: 181.1705; found: 181.1718. Elemental analysis calcd for $\text{C}_{47}\text{H}_{55}\text{N}_2\text{O}_4\text{P}$ (742.38): C, 75.98; H, 7.46; N, 3.77. Found: C, 74.10; H, 7.02; N, 4.05.

4.2.6. Synthesis of 14. DABCO (0.02 g, 0.2 mmol) was added to a clear solution of **1** (0.12 g, 0.2 mmol) in acetonitrile (20 mL) at room temperature and stirred for 10 h. The colorless precipitate thus obtained was collected by filtration and crystallized from a DMF and CH_3OH mixture at room temperature to obtain pure crystals of **14**, which were suitable for single-crystal X-ray diffraction analysis. Yield: 0.11 g, 74%. m.p.: 270 °C. ^1H NMR ($\text{CDCl}_3 + 0.1$ mL DMF, 25 °C): δ = 8.13 (s, 16H), 7.81 (DMF), 7.49 (s, 12H), 6.88–7.00 (m, 26H), 6.37 (s, 2H), 6.26 (s, 2H), 3.00 (br, DMF), 2.90 (s, DMF), 2.77 (s, DMF), 2.54 (DMF), 2.44 (s, DMF), 1.89 (s, 3H) ppm. ^{13}C NMR ($\text{CDCl}_3 + 0.1$ mL DMF, 75.431 MHz, 25 °C): 162.0 (DMF), 129.1, 127.4, 126.4, 51.3, 46.1, 45.2, 44.2, 40.0, 39.0, 35.9 (DMF), 33.8, 32.8, 30.8 (DMF), 27.7, 26.8, 21.5, 20.6, 15.4 ppm. $^{31}\text{P}\{^1\text{H}\}$ NMR ($\text{CDCl}_3 + 0.1$ mL DMF, 121.442 MHz, 25 °C): δ = -4.6 ppm. CP-MAS $^{31}\text{P}\{^1\text{H}\}$ NMR (163.32 MHz, 298 K): δ = -2.7, -4.2, and -6.9 ppm. IR (KBr pellet, cm^{-1}): $\bar{\nu}$ = 3425 (vs, br), 3082 (w), 3057 (w), 3025 (w), 2956 (w), 2384 (w, br), 2299 (w, br), 1631 (w), 1598 (w), 1493 (m), 1461 (m), 1445 (m), 1323 (w), 1291 (w), 1206 (m), 1178 (m), 1130 (w), 1056 (s), 1032 (w), 1002 (w), 922 (w), 877 (w), 850 (w), 787 (w), 765 (w), 749 (w), 702 (vs), 677 (w), 617 (m), 604 (m), 580 (w), 566 (w), 532 (w). ESI-MS: calcd (m/z) for $[\text{C}_{33}\text{H}_{28}\text{O}_4\text{P}]^-$: 519.1725; found: 519.1721. Elemental analysis calcd (%) for $\text{C}_{43}\text{H}_{53}\text{N}_3\text{O}_6\text{P}$: C, 69.90; H, 7.23; N, 5.69; found: C 70.20, H 6.49, N 4.57.

4.2.7. Synthesis of 15. 4,4'-Bipyridyl (0.05 g, 0.3 mmol) was added to a turbid solution of **3** (0.36 g, 0.6 mmol) in acetonitrile (80 mL) at room temperature and stirred for 40 h. The colorless precipitate was collected by filtration and crystallized from a CH_3OH solution at room temperature to obtain pure crystals of **15**. Yield: 0.36 g, 92%. m.p.: 238 °C. ^1H NMR ($\text{CDCl}_3 + 0.1$ mL DMF, 25 °C): δ = 8.25 (s, 1H, $\text{P}-\text{OH}$), 8.24 (s, 1H, $\text{P}-\text{OH}$), 7.93 (s, 1H), 7.61 (DMF), 7.28 (s, 1H), 7.23 (d, 2H), 6.72–6.80 (m, 8H), 6.70–6.70 (m, 12H),

6.25 (s, 2H), 6.09 (s, 2H), 4.84 (br, 8H), 2.81 (s, 3H), 2.70 (s, 4H), 2.58 (s, DMF), 2.47 (s, DMF), 2.24 (s, 4H), 2.22 (s, 4H), 0.60 (d, 6H) ppm. ^{13}C NMR (CDCl_3 + 0.1 mL DMF, 75.431 MHz, 25 °C): 162.1 (DMF), 149.2, 146.1, 145.5, 143.6, 136.3, 129.2, 127.5, 126.6, 125.5, 121.4, 51.4, 49.3, 46.2, 45.3, 39.1, 35.1 (DMF), 33.9, 33.0, 31.5 (DMF), 27.8, 26.8, 23.5, 21.6, 20.7, 15.0 ppm. $^{31}\text{P}\{^1\text{H}\}$ NMR (CDCl_3 + 0.1 mL DMF, 121.442 MHz, 25 °C): $\delta = -4.2$ ppm. CP-MAS $^{31}\text{P}\{^1\text{H}\}$ NMR (163.32 MHz, 298 K): $\delta = -1.3, -4.3, \text{ and } -5.2$ ppm. IR (KBr pellet, cm^{-1}): $\bar{\nu} = 3426$ (w, br), 3083 (w), 3026 (w), 2959 (m), 2869 (w), 2389 (w, br), 1632 (m), 1600 (m), 1494 (m), 1467 (w), 1447 (m), 1384 (w), 1363 (w), 1319 (w), 1259 (w), 1204 (w), 1160 (w), 1204 (m), 1160 (m), 1123 (m), 1077 (m), 1031 (w), 937 (s), 893 (m), 853 (w), 809 (m), 765 (w), 745 (w), 701 (vs), 648 (w), 633 (w), 606 (m), 591 (w), 590 (w), 565 (w), 524 (w). ESI-MS: calcd (m/z) for $[\text{C}_{35}\text{H}_{32}\text{O}_4\text{P}]^-$ 547.2038; found: 547.2030 and calcd (m/z) for $[\text{C}_{10}\text{H}_9\text{N}_2]^+$ 157.0766; found: 157.0817. Elemental analysis calcd (%) for $\text{C}_{83}\text{H}_{86}\text{N}_2\text{O}_{11}\text{P}_2$: C, 73.87; H, 6.42; N, 2.08; found: C 71.75, H 5.73, N 2.60.

4.2.8. Synthesis of 16. Anhydrous MgCl_2 (0.02 g, 0.2 mmol) was added to a turbid solution of **2** (0.22 g, 0.4 mmol) in acetonitrile (40 mL) at room temperature. After 5 min, Et_3N (0.14 mL, 1 mmol) was added. After stirring for half an hour, 3 mL of DMF was added and the stirring was continued for 24 h. The resulting colorless precipitate was collected by filtration of the reaction mixture and crystallized from a DMF and CH_3CN mixture at room temperature to obtain pure **16**. Yield: 0.15 g, 51%. m.p.: 124 °C. ^1H NMR (CDCl_3 , 25 °C): $\delta = 7.87$ (s, br, 6H), 7.42 (m, br, 2H), 7.33 (m, 2H, Ar-H), 7.22 (m, 2H, Ar-H), 6.95 (br, 54H), 6.74–6.85 (m, 22H), 6.51–6.66 (m, 17H), 6.29 (br, 6H), 6.14–6.20 (m, 3H), 5.85–5.90 (m, 2H), 5.78 (s, 1H), 3.30 (br, 14H), 2.72 (d, 37H), 2.51 (m, 7H), 2.32 (m, 6H), 1.18 (t, 3H), 1.10 (t, 3H), 0.95 (t, 10H) ppm. ^{13}C NMR (CDCl_3 , 75.431 MHz, 25 °C): 143.9 (Ar- C_{quart}), 129.6 (Ar- C_{quart}), 128.5 (Ar-CH), 127.9 (Ar-CH), 125.7 (Ar-CH), 49.7 (CHPh_2), 36.5 (DMF), 31.4 (DMF), 28.3 (CH_2CH_3), 15.5 (CH_2CH_3) ppm. $^{31}\text{P}\{^1\text{H}\}$ NMR (CDCl_3 , 121.442 MHz, 25 °C): $\delta = -4.9, -6.1, -8.2, -8.7, -10.4$ ppm. CP-MAS $^{31}\text{P}\{^1\text{H}\}$ NMR (163.32 MHz, 298 K): $\delta = -5.6$ ppm. IR (KBr pellet, cm^{-1}): $\bar{\nu} = 3423$ (s, br), 3084 (w), 3059 (m), 3026 (m), 2963 (m), 2932 (w), 2872 (w), 2390 (w, br), 1657 (s), 1600 (m), 1494 (m), 1447 (m), 1385 (w), 1321 (w), 1253 (m), 1203 (m), 1128 (m), 1103 (m), 1078 (m), 1032 (w), 1003 (w), 941 (s), 924 (s), 891 (m), 859 (w), 831 (w), 797 (w), 763 (w), 748 (w), 714 (s), 701 (vs), 622 (w), 605 (w), 584 (w), 561 (w), 514 (w). ESI-MS: calcd (m/z) for $[\text{C}_{40}\text{H}_{44}\text{MgN}_2\text{O}_6\text{P}]^+$ 703.2787; found: 703.2758 and calcd (m/z) for $[\text{C}_{68}\text{H}_{61}\text{MgO}_8\text{P}_2]^+$ 1091.3692; found: 1091.3810. Elemental analysis calcd (%) for $\text{C}_{77}\text{H}_{87}\text{MgN}_3\text{O}_{14}\text{P}_2$: C, 67.76; H, 6.43; N, 3.08; found: C 67.64, H 6.28, N 2.94.

4.2.9. Synthesis of 17. Anhydrous MgCl_2 (0.03 g, 0.3 mmol) was added to a turbid solution of **3** (0.36 g, 0.6 mmol) in acetonitrile (60 mL) at room temperature. After 5 min, Et_3N (0.25 mL, 1.8 mmol) was added. After stirring for half an hour, 6 mL of DMF was added and stirring was continued for 24 h. The resulting colorless precipitate was collected by filtering the reaction mixture and crystallized from a DMF and CH_3CN mixture at room temperature to obtain pure **17**. Yield: 0.23 g, 53%. m.p.: 194 °C. ^1H NMR (CDCl_3 , 25 °C): $\delta = 7.90$ (s, 4H, DMF), 7.44 (m, 2H), 7.32 (m, 2H, Ar-H), 7.20–7.27 (m, 4H, Ar-H), 6.99–7.11 (m, br, 12H), 6.89–6.96 (m, 16H, Ar-H), 6.82–6.85 (m, 8H, Ar-H), 6.73–6.81 (m, 14H, Ar-H),

6.49–6.69 (m, 20H, Ar-H), 6.14–6.21 (m, 4H), 5.93 (m, 1H), 5.79–5.83 (m, 2H), 3.14 (br, 11H), 2.76 (s, 14H), 2.70 (s, 14H), 1.07–1.18 (m, 17H), 0.94–0.99 (br, 4H), 0.86 (d, 1H) ppm. ^{13}C NMR (CDCl_3 , 75.431 MHz, 25 °C): 162.8, 147.2, 147.1, 145.6, 145.2, 145.1, 143.3, 143.2, 142.9, 142.5, 142.3, 137.5, 137.0, 136.2, 135.5, 130.3, 129.7, 129.5, 129.1, 128.7, 128.5, 128.3, 128.1, 127.8, 127.7, 126.2, 125.6, 125.4, 125.2, 50.4, 49.6, 49.0, 36.5 (DMF), 33.7, 33.4, 31.4 (DMF), 24.4 ($\text{CH}(\text{CH}_3)_2$), 24.3 ($\text{CH}(\text{CH}_3)_2$), 23.9 ($\text{CH}(\text{CH}_3)_2$), 23.8 ($\text{CH}(\text{CH}_3)_2$) ppm. $^{31}\text{P}\{^1\text{H}\}$ NMR (CDCl_3 , 121.442 MHz, 25 °C): $\delta = -4.9, -6.2, -8.4, -8.7, -10.4$ ppm. CP-MAS $^{31}\text{P}\{^1\text{H}\}$ NMR (163.32 MHz, 298 K): $\delta = -0.5$ and -8.8 ppm. IR (KBr pellet, cm^{-1}): $\bar{\nu} = 3423$ (s, br), 3083 (w), 3059 (w), 3026 (w), 2959 (m), 2869 (w), 2392 (w), 1951 (w), 1886 (w), 1657 (s), 1600 (w), 1493 (m), 1467 (w), 1446 (m), 1384 (w), 1362 (w), 1320 (w), 1256 (w), 1206 (m), 1162 (m), 1106 (m), 1079 (m), 1031 (w), 928 (m), 853 (w), 829 (w), 795 (w), 764 (w), 716 (s), 701 (vs), 669 (w), 648 (w), 632 (w), 621 (w), 591 (w), 573 (w), 527 (w). ESI-MS: calcd (m/z) for $[\text{C}_{70}\text{H}_{65}\text{MgO}_8\text{P}_2]^+$ 1119.4005; found: 1119.4050. Elemental analysis calcd (%) for $\text{C}_{82}\text{H}_{102}\text{MgN}_4\text{O}_{17}\text{P}_2$: C, 65.57; H, 6.85; N, 3.73; found: C 64.81, H 6.06, N 2.53.

■ ASSOCIATED CONTENT

Supporting Information

The Supporting Information is available free of charge on the ACS Publications website at DOI: 10.1021/acsomega.8b03192.

Solution- and solid-state NMR spectra; Hirshfeld surfaces; 2D fingerprint plots; contributions of different interactions; quantitative measures of volume (VH), area (SH), globularity (G), and asphericity; topology of the H-networks; and crystallographic details (PDF)

Crystallographic information files (CIF)

■ AUTHOR INFORMATION

Corresponding Authors

*E-mail: sbiswas@iitg.ac.in (S.B.).

*E-mail: carola.schulzke@uni-greifswald.de (C.S.).

*E-mail: vc@iitk.ac.in (V.C.).

*E-mail: scheschkewitz@mx.uni-saarland.de (D.S.).

*E-mail: ajana@tifrh.res.in (A.J.).

ORCID

Pankaj Kalita: 0000-0002-1240-5633

Vadapalli Chandrasekhar: 0000-0003-1968-2980

David Scheschkewitz: 0000-0001-5600-8034

Anukul Jana: 0000-0002-1657-1321

Notes

The authors declare no competing financial interest.

■ ACKNOWLEDGMENTS

This work was supported by the TIFR Centre for Interdisciplinary Sciences Hyderabad, Hyderabad, India. V.C. acknowledges the Department of Science and Technology, New Delhi, India, for a National J. C. Bose fellowship. The authors thank Pawan Kumar and Joydev Acharya, Department of Chemistry, IIT Kanpur, Kanpur, India, for their help in obtaining the high-resolution mass spectrometry and elemental analysis data. We are also thankful to Prof. Shaikh M. Mobin and SIC, IIT Indore, for the single-crystal X-ray data of compounds **16** and **17**.

REFERENCES

- (1) Bhosale, R. S.; Kobaisi, M. A.; Bhosale, S. V.; Bhargava, S.; Bhosale, S. V. Flower-like supramolecular self-assembly of phosphonic acid appended naphthalene diimide and melamine. *Sci. Rep.* **2015**, *5*, No. 14609.
- (2) Desiraju, G. R.; Vittal, J. J.; Ramanan, A. *Crystal Engineering: A Textbook*; World Scientific: Singapore, 2011.
- (3) Desiraju, G. R.; Steiner, T. *The Weak Hydrogen Bond in Structural Chemistry and Biology*; Oxford University Press: Oxford, U.K., 1999.
- (4) Korhonen, H. J.; Conway, L. P.; Hodgson, D. R. W. Phosphate analogues in the dissection of mechanism. *Curr. Opin. Chem. Biol.* **2014**, *21*, 63–72.
- (5) Parmar, D.; Sugiono, E.; Raja, S.; Rueping, M. Complete Field Guide to Asymmetric BINOL-Phosphate Derived Brønsted Acid and Metal Catalysis: History and Classification by Mode of Activation; Brønsted Acidity, Hydrogen Bonding, Ion Pairing, and Metal Phosphates. *Chem. Rev.* **2014**, *114*, 9047–9153.
- (6) Zamfir, A.; Schenker, S.; Freund, M.; Tsogoeva, S. B. Chiral BINOL-derived phosphoric acids: privileged Brønsted acid organocatalysts for C–C bond formation reactions. *Org. Biomol. Chem.* **2010**, *8*, 5262–5276.
- (7) Reid, J. P.; Goodman, J. M. Selecting Chiral BINOL-derived Phosphoric Acid Catalysts: General Model to Identify Steric Features Essential For Enantioselectivity. *Chem. – Eur. J.* **2017**, *23*, 14248–14260.
- (8) Akiyama, T. Stronger Brønsted acids. *Chem. Rev.* **2007**, *107*, 5744–5758.
- (9) Champagne, P. A.; Houk, K. N. Origins of Selectivity and General Model for Chiral Phosphoric Acid-Catalyzed Oxetane Desymmetrizations. *J. Am. Chem. Soc.* **2016**, *138*, 12356–12359.
- (10) Liao, S.; Leutzsch, M.; Monaco, M. R.; List, B. Catalytic enantioselective conversion of epoxides to thiiranes. *J. Am. Chem. Soc.* **2016**, *138*, 5230–5233.
- (11) Monaco, M. R.; Fazzi, D.; Tsuji, N.; Leutzsch, M.; Liao, S.; Thiel, W.; List, B. The Activation of Carboxylic Acids via Self-Assembly Asymmetric Organocatalysis: A Combined Experimental and Computational Investigation. *J. Am. Chem. Soc.* **2016**, *138*, 14740–14749.
- (12) Huang, S.; Kötzner, L.; De, C. K.; List, B. Catalytic Asymmetric Dearomatizing Redox Cross Coupling of Ketones with Aryl Hydrazines Giving 1,4-Diketones. *J. Am. Chem. Soc.* **2015**, *137*, 3446–3449.
- (13) Müller, S.; Webber, M. J.; List, B. The catalytic asymmetric Fischer indolization. *J. Am. Chem. Soc.* **2011**, *133*, 18534–18537.
- (14) Zi, W.; Wang, Y.-M.; Toste, F. D. An In Situ Directing Group Strategy for Chiral Anion Phase-Transfer Fluorination of Allylic Alcohols. *J. Am. Chem. Soc.* **2014**, *136*, 12864–12867.
- (15) Phipps, R. J.; Hamilton, G. L.; Toste, F. D. The progression of chiral anions from concepts to applications in asymmetric catalysis. *Nat. Chem.* **2012**, *4*, 603–614.
- (16) Avila, C. M.; Patel, J. S.; Reddi, Y.; Saito, M.; Nelson, H. M.; Shunatona, H. P.; Sigman, M. S.; Sunoj, R. B.; Toste, F. D. Enantioselective Heck–Matsuda Arylations through Chiral Anion Phase-Transfer of Aryl Diazonium Salts. *Angew. Chem., Int. Ed.* **2017**, *56*, 5806–5811.
- (17) Dar, A. A.; Mallick, A.; Murugavel, R. Synthetic strategies to achieve further-functionalised monoaryl phosphate primary building units: crystal structures and solid-state aggregation behavior. *New J. Chem.* **2015**, *39*, 1186–1195.
- (18) Kalita, A. C.; Sharma, K.; Murugavel, R. Pseudopolymorphism leading and two different supramolecular aggregations in a phosphate monoester: role of a rare water-dimer. *CrystEngComm* **2014**, *16*, 51–55.
- (19) Kuczek, M.; Bryndal, I.; Lis, T. 4-Nitrophenyl phosphoric acid and its four different potassium salts: a solid state structure and kinetic study. *CrystEngComm* **2006**, *8*, 150–162.
- (20) Lazar, A. N.; Dupont, N.; Navaza, A.; Coleman, A. W. Solid-state complexes of calix [4] arene dihydroxyphosphonic acid with bipyridyl ligands. *Cryst. Growth Des.* **2006**, *6*, 669–674.
- (21) Lazar, A. N.; Navaza, A.; Coleman, A. W. Solid-state caging of 1,10-phenanthroline π – π stacked dimers by calix[4]arene dihydroxyphosphonic acid. *Chem. Commun.* **2004**, *0*, 1052–1053.
- (22) Wang, X.-Z.; Yao, Z.-J.; Liu, H.; Zhang, M.; Yang, D.; George, C.; Burke, T. R. Synthesis of a phosphotyrosyl analogue having χ_1 , χ_2 and φ angles constrained to values observed for an SH2 domain-bound phosphotyrosyl residue. *Tetrahedron* **2003**, *59*, 6087–6093.
- (23) Onoda, A.; Yamada, Y.; Okamura, T.; Yamamoto, H.; Ueyama, N. Mononuclear Ca (II)-Bulky Aryl Phosphate Monoanion and Dianion Complexes with Ortho-Amide Groups. *Inorg. Chem.* **2002**, *41*, 6038–6047.
- (24) Onoda, A.; Okamura, T.-a.; Yamamoto, H.; Ueyama, N. One-dimensional P–OH...O=P hydrogen bonds restricted by the bulky molecule 2, 6-diisopropylphenyl dihydrogen phosphate. *Acta Crystallogr., Sect. E: Struct. Rep. Online* **2001**, *57*, o1022–o1024.
- (25) Ianeli, S.; Nardelli, M.; et al. Hydrogen-Bonding Stabilization of N-Methyl-dopamine 4-O-Dihydrogenphosphate in HCl Acidic Solution: Synthesis of Z2055, a New Dopaminergic Prodrug. *Acta Crystallogr., Sect. C: Cryst. Struct. Commun.* **1995**, *51*, 1338–1341.
- (26) Mandal, D.; Santra, B.; Kalita, P.; Chrysochos, N.; Malakar, A.; Narayanan, R. S.; Biswas, S.; Schulzke, C.; Chandrasekhar, V.; Jana, A. 2,6-(Diphenylmethyl)-Aryl-Substituted Neutral and Anionic Phosphates: Approaches to H-Bonded Dimeric Molecular Structures. *ChemistrySelect* **2017**, *2*, 8898–8910.
- (27) Saxena, P.; Mandal, S. K.; Sharma, K.; Murugavel, R. Delineating factors that dictate the framework of a bulky phosphate derived metal complexes: Sterics of phosphate, anion of the metal salt and auxiliary N-donor ligand. *Inorg. Chim. Acta* **2018**, *469*, 353–365.
- (28) Dhara, D.; Vijayakanth, T.; Barman, M. K.; Naik, K. P. K.; Chrysochos, N.; Yildiz, C. B.; Boomishankar, R.; Schulzke, C.; Chandrasekhar, V.; Jana, A. NHC-stabilized 1-hydrosilamine: synthesis, structure and reactivity. *Chem. Commun.* **2017**, *53*, 8592–8595.
- (29) Dhara, D.; Kalita, P.; Mondal, S.; Narayanan, R. S.; Mote, K. R.; Huch, V.; Zimmer, M.; Yildiz, C. B.; Scheschke, D.; Chandrasekhar, V.; Jana, A. Reactivity Enhancement of a Diphosphene by Reversible N-Heterocyclic Carbene Coordination. *Chem. Sci.* **2018**, 4235–4243.
- (30) Bourissou, D.; Guerret, O.; Gabbai, F. P.; Bertrand, G. Stable carbenes. *Chem. Rev.* **2000**, *100*, 39–92.
- (31) Cowan, J. A.; Clyburne, J. A. C.; Davidson, M. G.; Harris, R. L. W.; Howard, J. A. K.; Küpper, P.; Leech, M. A.; Richards, S. P. On the Interaction between N-Heterocyclic Carbenes and Organic Acids: Structural Authentication of the First N–H...C Hydrogen Bond and Remarkably Short C–H...O Interactions. *Angew. Chem., Int. Ed.* **2002**, *41*, 1432–1434.
- (32) Kuhn, N.; Kratz, T. Synthesis of imidazol-2-ylidenes by reduction of imidazole-2 (3H)-thiones. *Synthesis* **1993**, 561–562.
- (33) Gusev, D. G. Electronic and Steric Parameters of 76 N-Heterocyclic Carbenes in Ni(CO)₃(NHC). *Organometallics* **2009**, *28*, 6458–6461.
- (34) Ghadwal, R. S.; Azhakar, R.; Roesky, H. W.; Pröpper, K.; Dittrich, B.; Goedecke, C.; Frenking, G. Donor–acceptor stabilized silylformyl chloride. *Chem. Commun.* **2012**, *48*, 8186–8188.
- (35) Merckens, C.; Pana, F.; Englert, U. 3-(4-Pyridyl)-2,4-pentanedione—a bridge between coordinative, halogen, and hydrogen bonds. *CrystEngComm* **2013**, *15*, 8153–8158.
- (36) Mote, N. R.; Patel, K.; Shinde, D. R.; Gaikwad, S. R.; Koshti, V. S.; Gonnade, R. G.; Chikkali, S. H. H-Bonding Assisted Self-Assembly of Anionic and Neutral Ligand on Metal: A Comprehensive Strategy To Mimic Ditopic Ligands in Olefin Polymerization. *Inorg. Chem.* **2017**, *56*, 12448–12456.
- (37) Takase, M.; Inouye, M. Highly efficient recognition of native TpT by artificial ditopic hydrogen-bonding receptors possessing a conformationally well-defined linkage. *J. Org. Chem.* **2003**, *68*, 1134–1137.

(38) Yun, J. W.; Tanase, T.; Lippard, S. J. Carboxylate- and Phosphate Ester-Bridged Dimagnesium(II), Dizinc(II), and Dicalcium(II) Complexes. Models for Intermediates in Biological Phosphate Ester Hydrolysis. *Inorg. Chem.* **1996**, *35*, 7590–7600.

(39) Murugavel, R.; Kuppaswamy, S.; Randoll, S. Cooperative Binding of Phosphate Anion and a Neutral Nitrogen Donor to Alkaline-Earth Metal Ions. Investigation of Group 2 Metal–Organophosphate Interaction in the Absence and Presence of 1,10-Phenanthroline. *Inorg. Chem.* **2008**, *47*, 6028–6039.

(40) Paschoal, V. H.; Faria, L. F. O.; Ribeiro, M. C. C. Vibrational Spectroscopy of Ionic Liquids. *Chem. Rev.* **2017**, *117*, 7053–7112.

(41) Lassègues, J.-C.; Grondin, J.; Cavagnat, D.; Johansson, P. New Interpretation of the CH Stretching Vibrations in Imidazolium-Based Ionic Liquid. *J. Phys. Chem. A* **2009**, *113*, 6419–6421.